Ultrasound Analysis of the Most Important Musculoskeletal Issues

Dan Tschanz[1] and Paolo Lombardo[1]

[1]Department of Diagnostic, Interventional and Pediatric Radiology (DIPR), Inselspital, Bern University Hospital, University of Bern, Switzerland

[1] Corresponding author: Dan Tschanz - received: 20.05.2024 - peer reviewed and published: 15.06.2024

Contents

1. Abstract

This work shows the most important standard sections of relevant questions in musculoskeletal (MSK) ultrasound of the wrist, elbow, shoulder, hip, knee and ankle. Exemplary images with descriptions of the sections and anatomical structures were created and the positioning of the patient explained. Several patient cases per region were also presented and explained in order to place the described procedures in a clinical context. The advantages and disadvantages of the imaging procedures were explained and compared.

MSK ultrasound is particularly strong in the visualisation of superficial structures, whereby this form of imaging is superior to other imaging procedures in some cases. In addition, the detection of inflammation, for example, is not only possible via indirect signs (e.g. free fluid or abscess) compared to computer tomography. In addition, the hyperperfusion caused by inflammation can be visualised directly at the affected site using Doppler examination.

Even in the case of functional restrictions such as shoulder impingement or tendon instability (see section 4.6.11: Patient case 19), which are difficult to visualise using other imaging techniques, the tissue can be viewed and moved in vivo using a dynamic examination. This can lead to a better understanding of the pathology and a more precise diagnosis. MSK sonography therefore proves to be a valuable addition to everyday clinical practice.

The focus of our work was the presentation of common standard ultrasound incisions in the MSK area. The intention to keep this guide clear and to cover the common pathologies is limited by the fact that not all sections could be covered. In a future work, further, less frequently used incisions could be shown in order to cover a broader spectrum of possible pathologies. For example, sections of the thorax (such as the thoracolumbar fascia or areas of the spine and lumbar region) could also be shown.

A further question is whether MSK ultrasound can save or replace an MRI or CT examination in certain cases. As discussed in the introduction, this would be an advantage from the patient's point of view and in economic terms. Further studies investigating this aspect would be valuable.

---

2. Introduction

Ultrasound has established itself as a diagnostic imaging technique in medicine over the last few decades and has undergone continuous further development. This form of imaging is particularly valued due to the negligible health risk for patients, but also for its rapid availability, cost-effectiveness and the possibility of viewing the tissue in vivo in terms of dynamic examination or using Doppler flow visualisation, for example.

The use of musculoskeletal ultrasound (hereafter MSK ultrasound) has risen sharply. A study from the USA showed that between 2000 and 2009, the use of MSK ultrasound increased by 316% overall (from 56,254 examinations in 2000 to 233,964 in 2009) and in private practices by as much as 717% (from 19,372 examinations in 2000 to 233,964 in 2009).[1]

Due to the various advantages (see section 2.2.1), the question arises as to whether similar growth would be desirable and cost-effective in Switzerland. Compared to magnetic resonance imaging (hereafter MRI) in particular, ultrasound may offer an alternative that is sufficient in many cases, and in some cases even superior, more rapidly available and cheaper.[2]

The aim of this paper is to explain the technique of MSK ultrasound to the reader using the wrist, elbow, shoulder, hip, knee and foot regions as examples. It is also intended to serve as a guide for practical everyday support. In each case, the positioning of the patient, the correct positioning of the ultrasound probe and the structures to be visualised are discussed. Several patient cases are presented as examples for each region.

To make it easier to understand the steps described, the left extremity is always shown in images and sonographically. The examination steps and images can be transferred to the right side in mirrored form.

The choice of colours is taken from the Inselspital's current (2023) colour scheme.

For reasons of readability and clarity, the masculine form is used in this document. However, all people are always meant in the same way.

3. Background

3.1. Physical basics

The formation of ultrasound images is based on the reflection of sound waves in the human body. A transducer generates sound waves in the range of several megahertz (MHz) via voltage changes on piezoelectric crystals. The sound waves are transmitted to the body via ultrasound gel, penetrate the tissue and are reflected in parts. The different tissues in the human body have different properties with regard to the speed of sound propagation (see Table 1) and therefore also differences in their impedance. As the average speed in different body tissues does not differ massively (except for bone and air), most devices calculate the depth of an echo with an average speed of 1540 m/s, without major distortions of the depth calculation being to be expected.[3]

The signals obtained in this way from several coplanar pulses are combined and processed to create an image. An ultrasound probe therefore acts as a loudspeaker and as a microphone as well.[4]

Echoes received earlier are displayed close to the transducer, while later received echoes are displayed further away from the transducer on the screen.[3]

Sound propagation in human tissues	
Air	331 m/s
Liver parenchyma	1549 m/s
Spleen parenchyma	1566 m/s
Muscle	1568 m/s
Bone	3360 m/s

Table 1 (taken from: Sono Grundkurs, Hofer M., 2023) [3]

3.2. Musculoskeletal ultrasound: strengths, limitations, area of application

3.2.1. Strengths

MSK ultrasound as a diagnostic imaging technique has many strengths. Nowadays, almost every hospital has at least one device, which is often equipped with a suitable linear probe. In contrast to the frequently prescribed MRI examination, no clarification for body implants is required here, which means that practically every patient is suitable for this type of imaging.[5]

Many patients are also unable to undergo an MRI examination because they suffer from claustrophobia. The development of open permanent magnet MRI systems has brought significant relief here, but a study conducted in 2007 (n=36) showed that 8.3% of examinations still had to be cancelled due to claustrophobia.[6]

Another study analysed patient satisfaction after an MRI versus an ultrasound examination for shoulder pain. All patients (n=118) would have been willing to repeat the ultrasound examination. Ten patients would have refused a second MRI examination. 93 patients preferred ultrasound, eight preferred MRI, and 17 patients reported no preference.[2]

Another advantage is the higher resolution. A 10 MHz probe has an axial resolution of around 150 µm.[7] With an MRI with a field strength of 1.5T, a field-of-view of 12x6 cm, a matrix of 256x256 pixels and a slice thickness of 0.5cm, a pixel size of 469µm can be achieved.[8]

In addition, a dynamic examination of the tissue is possible, which enables, for example, the diagnosis of subacromial impingement[9, 10], dislocation of the ulnar nerve[11] or subluxation of peroneal tendons[12].

There is great anatomical variance in the musculoskeletal system. It is therefore helpful to examine both sides in order to decide whether an abnormality is present or not. For example, the thickness of tendons can vary depending on their habitus, which can make it difficult to establish reference values and thus to decide whether a tendon is thickened or not. In contrast to MRI, it is easy to also examine the contralateral side during ultrasound examinations and thus obtain a comparative image.[5]

Although the sonographic visualisation of bone is limited, excellent reproduction of the anatomical details of the cortical surface of superficial bone is possible. The high resolution enables the detection and assessment of small changes, some of which are not visible in a conventional X-ray image, such as fractures of the scaphoid or Hills-Sachs lesions.[13]

For some examinations, MSK ultrasound has been shown to be equivalent to or better than MRI:

- Acute injuries of the lateral meniscus (sensitivity, US: 92.9% vs. MRI: 90.5%, specificity 88.9% vs. 83.9%, n=60)[14]
- Achilles tendon injuries (no significant difference)[15]
- Peripheral nerve injuries (sensitivity for structural interruption or change in calibre, US: 100% vs MRI: 70%, or 100% vs. 50%)[16]
- Chronic lateral epicondylitis (no significant difference; $\kappa = 0.49$)[17]

3.2.2. Limitations

Despite the many strengths of MSK ultrasound, there are some relevant limitations:

- X-ray and computed tomography (CT) have a much better representation of bone mineralisation and spatial representation of fractures.
- MRI is superior to ultrasound in the imaging of bone marrow, bone tumours, joints and muscles that are not accessible to high-frequency ultrasound probes (e.g. spine, cruciate ligaments, sacroiliac ligaments).
- Ultrasound generates artefacts that do not occur in this way with other examination methods (for example, anisotropy in the visualisation of tendons, see section 3.1.1).
- The quality of the examination is highly dependent on the examiner, as it requires a great deal of expertise and background knowledge as well as practice. [18]
- Due to large impedance jumps, the sound waves are completely reflected (for example in bones or air). This means that underlying structures cannot be visualised. A lower transmission frequency must also be selected to visualise deep structures, which reduces the image resolution.

3.3. Reasons for a standardised examination technique

Ultrasound is considered to be examiner-dependent, as the probe can be positioned in any arbitrary position, rotation, angulation and tilt on the patient. The question therefore arises as to how reliable the assessment and interpretation of a finding is and whether a different examiner would make the same diagnosis.

In order to enable comparable results and clearly interpretable findings, it is necessary to define standard section levels in order to reliably record the relevant and frequent pathologies and to document them in a way that is comprehensible to other specialists.

4. Musculoskeletal ultrasound in general

4.1. Performance of an MSK Ultrasound

MSK ultrasound refers to the sonographic examination of tendons, muscles, nerves, soft tissue and bone surfaces.[19]

To carry out an ultrasound examination, an ultrasound device equipped with a suitable probe is required. In the MSK range, a linear probe, usually in the 5-13 MHz range, is generally used. For deeper structures or in obese patients, it may be advisable to use a lower- frequency convex probe to achieve the necessary depth.[20]

Ultrasound gel is applied to the structure to be examined, which transmits the sound waves from the probe to the target tissue. Gel pads can also be used to minimise artefacts (e.g. due to compression). The region is palpated to localise anatomical landmarks. It is important that the examiner has a detailed and precise understanding of the local anatomy in order to achieve optimal positioning of the probe. The ultrasound probe is placed perpendicular to the surface, with the probe indicator pointing cranially or to the right from the patient's perspective. This allows a standardised visualisation of the organs to be achieved.[20]

Normally, the structures to be analysed are shown in longitudinal and transverse axes, with the longest extension of the structure serving as the reference in each case. If the organ lies in a body axis, this is used to describe the positioning. For example, a sagittal section is used for the longitudinal section of the tendon of the biceps caput longum, as this corresponds to the longitudinal section of the tendon. If this is not the case, the terms "longitudinal section" and "transverse section" are used.[20]

The examined region is displayed on the screen in real time and can be assessed by the examiner. Images and video recordings are normally saved and can be viewed again at a later date or sent as an attachment to a report.

4.2. Most important artefacts

As with all imaging procedures, the image shown on the monitor does not always reflect reality. There are so-called artefacts that need to be recognised. The artefacts most frequently encountered in the MSK area are described below.

4.2.1. Anisotropy

Anisotropy is one of the most common and therefore probably the most important artefact of MSK ultrasound. It describes the change in the displayed echogenicity of normal tissue when the sonication angle deviates from 90°. This effect is most pronounced in parallel-fibred structures such as tendons, less so in muscles, nerves or ligaments. A common location where this artefact occurs is when examining the supraspinatus tendon, as it has a curved course over the humeral head. A supposed reduction in echogenicity due to anisotropy should not be confused with an injury or even rupture of the tendon. To differentiate between artefact and pathology, the probe is tilted in place until the sound waves strike the tendon at a right angle. At this point, the image normalises if the tendon is intact. As an example, the iliopsoas tendon is shown here at two different sonication angles:[13]
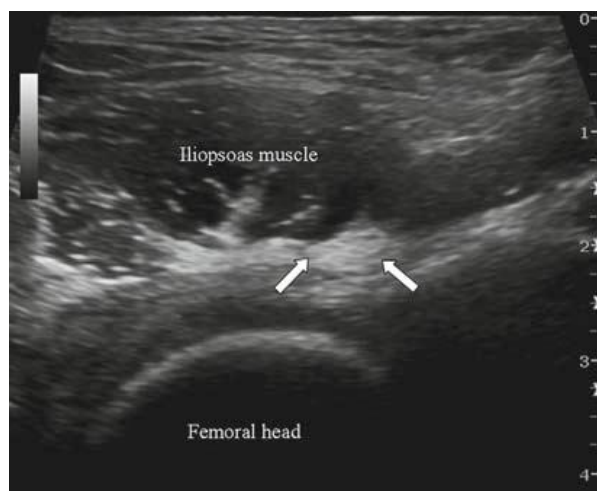

Figure 1: The iliopsoas tendon (arrows) shows a normal hyperechoic structure in transverse positioning oft he ultrasound probe. (Image source: O'Neill J., 2008) [13]
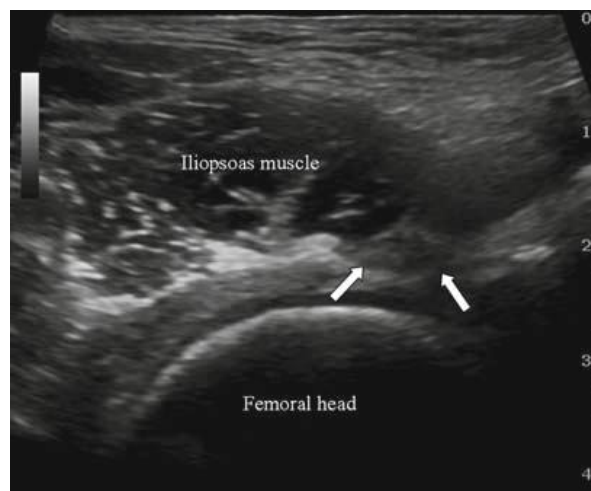

Figure 2: By tilting the probe by 5-10°, the tendon is visualised as hypoechoic and can be mistaken for pathology. (Image source: O'Neill J, 2008) [13]

4.2.2. Acoustic shadow

In most cases, only part of the sound energy is reflected during impedance discontinuities. However, in the case of large impedance jumps such as bone or air, almost all of the sound energy is reflected, which appears as an echo line. The sound shadow artefact can be observed in the corticalis sound head (Fig. 3, bottom right): An image strip of greatly reduced echogenicity.[3] As an example, a sagittal section of the Achilles tendon insertion (see Chapter 4.6.6, Fig. 130). In Fig. 3, top

Figure 3: Example of an acoustic shadow.

right, the echo line of the calcaneus can be seen, anterior to it (Fig. 3, bottom) the acoustic shadow. In contrast, there is no tissue proximally (Fig. 3, left) that would cause total reflection of sound. This makes it possible to visualise deeper structures such as the Kager fat body.
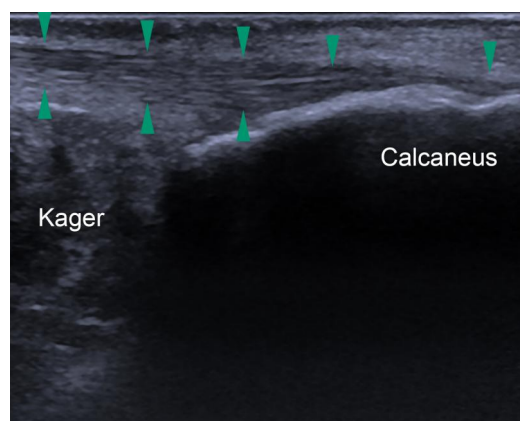
4.2.3. Reverberations

The calculation of the visual representation of the echoes assumes that the sound waves return directly from their reflection to the transducer. However, if several relevant impedance differences occur, reflected sound waves can be reflected again deeper into the tissue on their way back. At depth, they are reflected back again and finally reach the transducer. The increased propagation time allows the echo to be evaluated at a supposedly greater penetration depth. This can also happen several times: In this way, this can result in

Figure 4: Example for reverberations (green arrows).

several incorrectly drawn lines[3], such as here under the greater tuberosity of the humerus (longitudinal view of the infraspinatus tendon, see Chapter 4.1.4, Fig. 19).
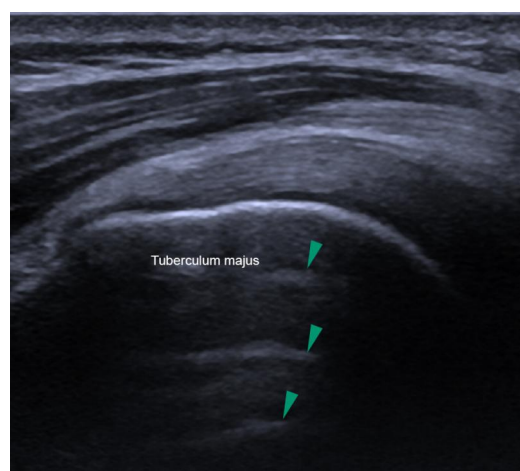
5. Systematic targeted investigations

5.1. Shoulder

Examination of the shoulder requires flexible positioning of the patient. A rotating chair is suitable for this, whereby the patient can be rotated slightly if necessary.[9]
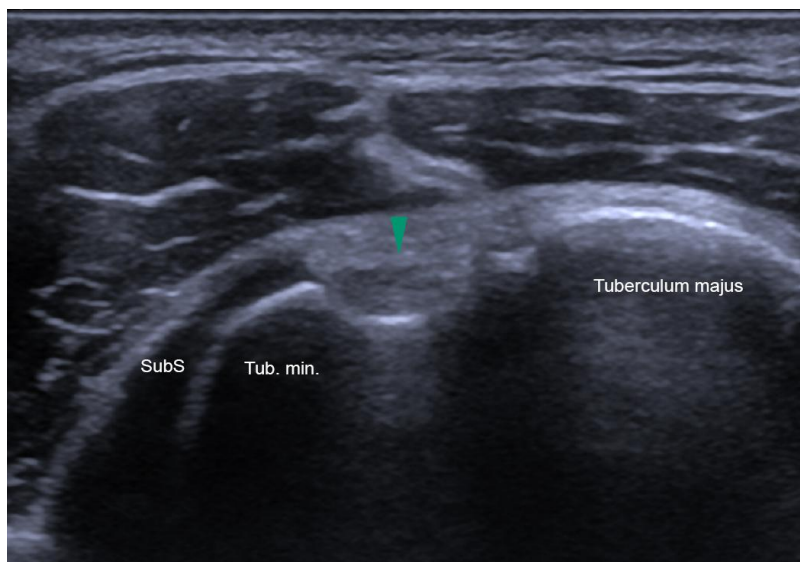
5.1.1. Biceps tendon

Figure 5: Cross-section of the biceps tendon. Green arrow: biceps tendon. Tub.min.: Tuberculum minus. SubS: subscapularis tendon.
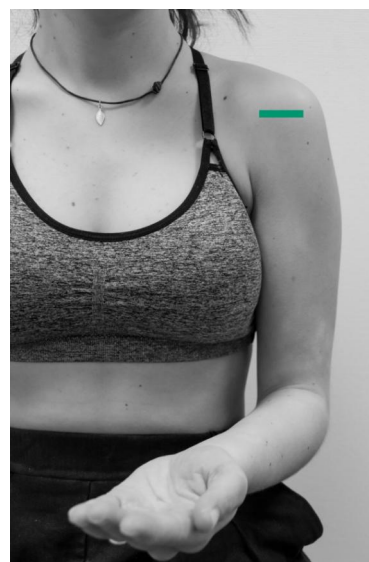

Figure 6: Probe positioning.

The examination of the shoulder begins with the biceps tendon. To do this, the patient should slightly internally rotate the arm to be examined, flex the elbow joint 90° and hold the forearm in a supinated position. The long biceps tendon can be found most easily between the lesser and greater tuberosities. It should be visualised and documented in its transverse and longitudinal axis.[9]
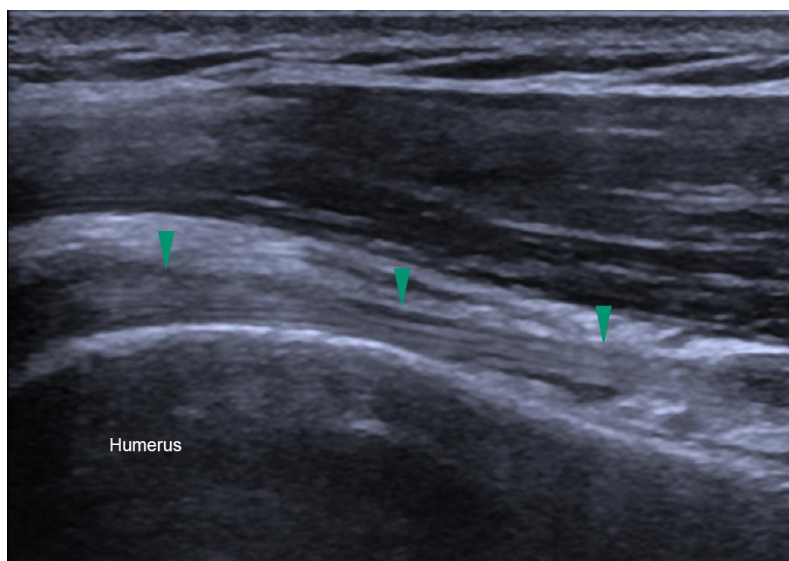

Figure 7: Longitudinal view of the biceps tendon. Green arrows: Biceps tendon.
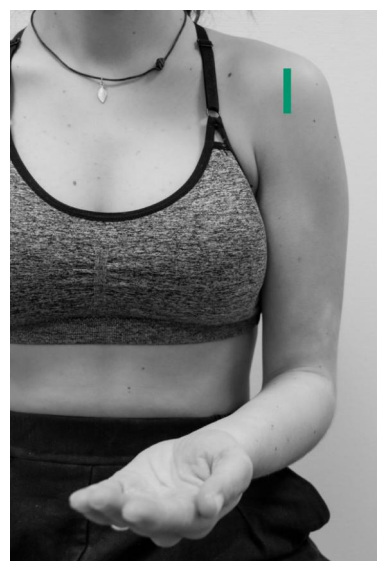

Figure 8: Probe positioning.
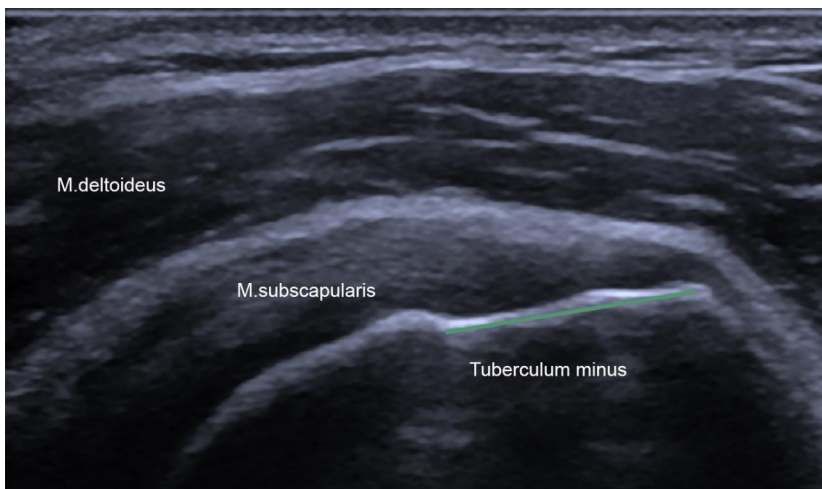
5.1.2. Subscapularis tendon

Figure 9: Longitudinal view of the subscapularis tendon. Green line: area of insertion of the subscapularis tendon.

Figure 10: Probe positioning..

To visualise the subscapularis tendon, the elbow joint is rotated outwards from the previous examination position. It is important to ensure that the elbow remains close to the patient's body, as otherwise the rotation is compensated for by extension of the elbow, which makes standardised imaging impossible. Supination is also maintained here. The probe is placed in the transverse plane in the position shown.[9]

The insertion of the subscapularis muscle can now be viewed at the level of the lesser tuberosity. A large part of this tendon can be visualised by slight passive internal and external rotation and by moving the probe proximally and distally. The tendon is visualised in cross-section by rotating the probe through 90°.[9]
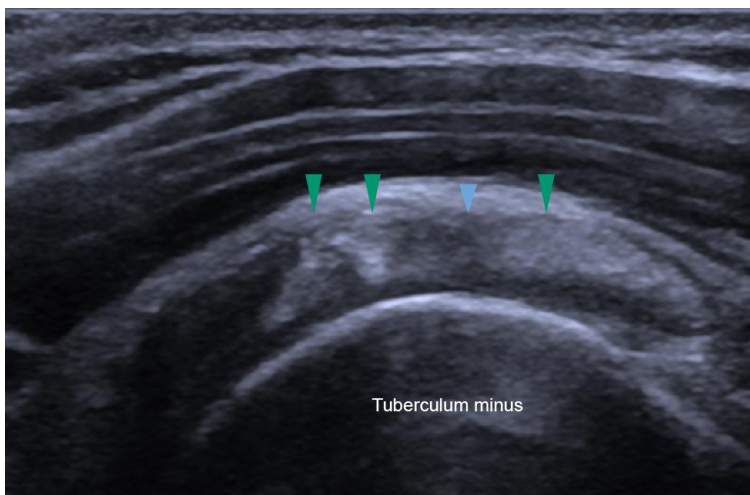

Figure 11: Longitudinal view oft he tendon of the subscapularis muscle. Green arrows: tendon fascicles of the subscapularis tendon. Blue arrow: muscle fibres embedded in the tendon.

Figure 12: Probe positioning.

5.1.3. Supraspinatus tendon

Figure 13: Patient positioning for the examination of the supraspinatus muscle.

To visualise the supraspinatus muscle, the back of the hand is placed on the opposite side of the back to achieve maximum internal rotation, with the elbow remaining in 90° flexion. It is important that the elbow is brought as close as possible to the thoracic wall.[9]

In this way, the fibres of the supraspinatus tendon are stretched, and a possible tear becomes more visible. At the same time, internal rotation shifts the tendon insertion anteriorly, making it easier to visualise.[9]

The easiest way to find the supraspinatus tendon is to first visualise the biceps tendon in the shoulder joint. A transverse section rotated clockwise by approx. 30° is used for this. As soon as the biceps tendon can be seen, it must be visualised in its longest extension, for which the transducer is rotated. If the biceps tendon is visible in its longest extension, the transducer can be moved cranially while maintaining the rotation. This ensures that the supraspinatus tendon is visualised in its longest axis (see next page).[9]

If the supraspinatus tendon is displayed, any anisotropy artefacts can be avoided by angulation. [9]
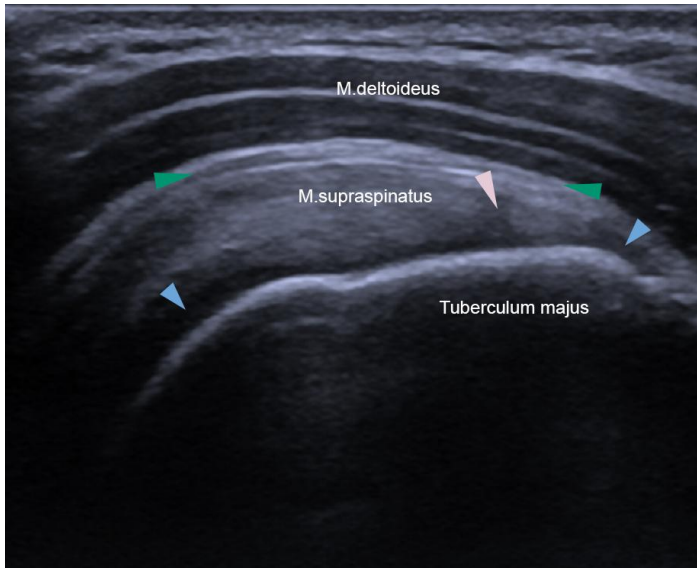
Figure 14: Supraspinatus tendon in longitudinal section. Green arrows: Subacromial subdeltoid bursa. Blue arrows: Articular cartilage. Pink arrow: Anisotropy (artefact)

Figure 15: Probe positioning for longitudinal view.

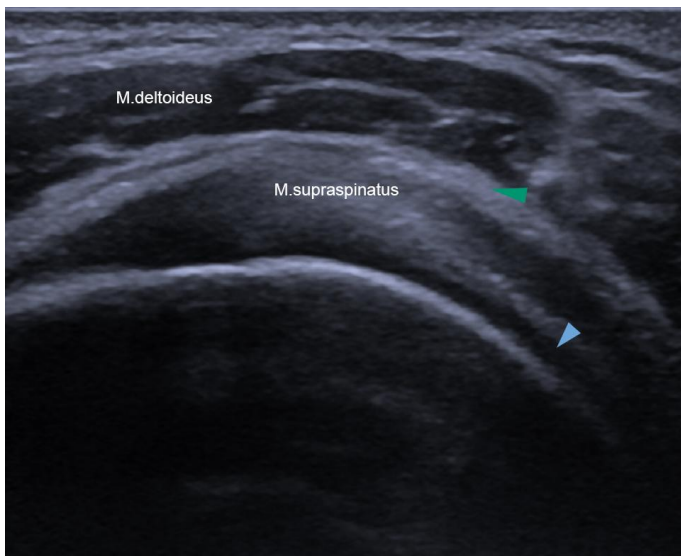By rotating the probe by 90°, the tendon can be visualised in cross-section and be examined in its course.[9]

Figure 16: Supraspinatus tendon in cross-section: Green arrow: Subacromial subdeltoid bursa. Blue arrow: articular cartilage.

Figure 17: Probe positioning for cross-section

5.1.4. Infraspinatus tendon

Figure 18: Patient positioning for the examination of the infraspinatus tendon.

To visualise the infraspinatus tendon, the patient is asked to place the hand of the limb to be examined on the opposite shoulder. This ensures better exposure of the tendon.[9]

The probe is placed dorsally in the presumed longitudinal axis of the infraspinatus muscle. It is advisable to use the spina scapulae as a landmark and to move the probe caudally from there under visualisation until the infraspinatus tendon can be seen in the image.[9]
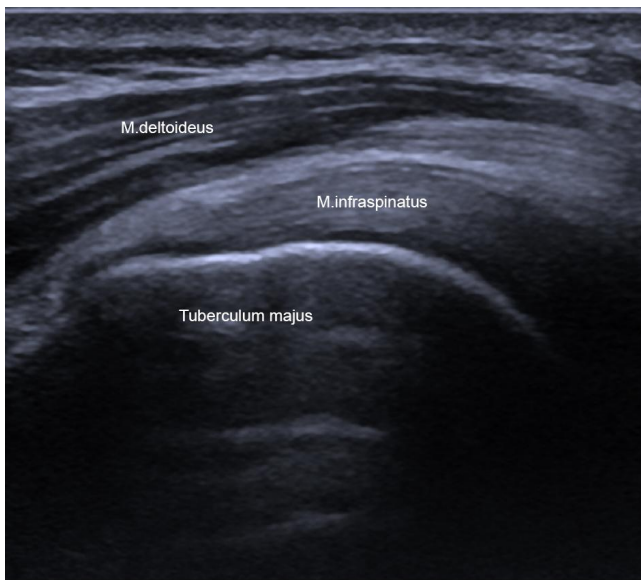

Figure 19: Longitudinal view of the infraspinatus tendon.

Figure 20: Probe positioning.

Note: if desired, the tendon of the teres minor can be visualised here by moving the probe further caudally.[9]

5.1.5. Acromioclavicular joint
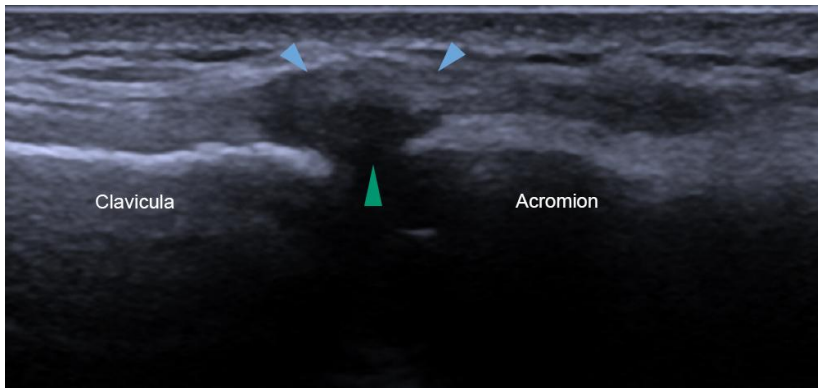

Figure 21: Longitudinal view of the AC joint. Green arrow: joint space. Blue arrows: Lig.acromioclaviculare superius

Figure 22: Probe positioning.

The AC joint can be examined in the coronal plane by positioning the transducer as shown. It is moved anteriorly and posteriorly to exclude or confirm the presence of an acromial bone. A possible joint effusion can also be visualised here.[9]

5.1.6. Patient case 1: Rupture of the long biceps tendon

A 40-year-old patient presented. When lifting a heavy object, he heard a snap in his left shoulder, causing the left biceps to bulge distally. The clinical presentation was a 'Popeye arm'. [21]

The subsequent ultrasound examination showed a complete rupture of the long biceps tendon, which could be demonstrated directly (discontinuity of the tendon) and indirectly (distalisation of the myotendinous junction of the biceps muscle, caput longus to below the insertion of the pectoralis tendon). The rotator cuff was intact.[21]
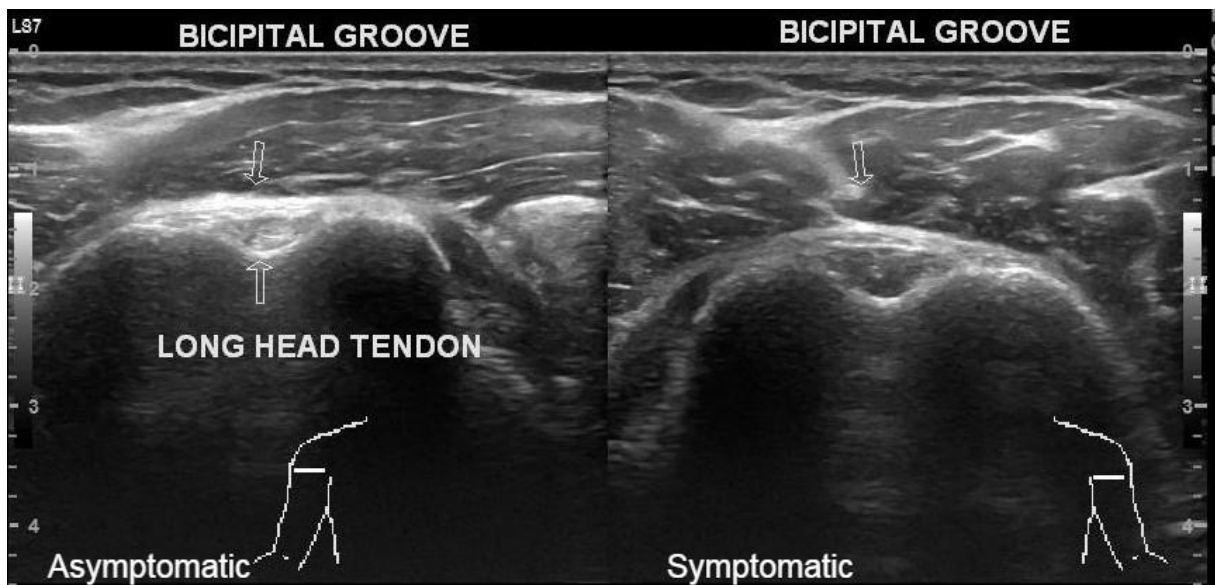

Figure 23: Cross-section of the biceps tendon: left of the asymptomatic side, right of the symptomatic side. (Image source: Stanislavsky A. et al., 2019, radiopaedia.org) [21]

Figure 24: Longitudinal section of the biceps tendon: left of the asymptomatic side, right of the symptomatic side. (Image source: Stanislavsky A. et al., 2019, radiopaedia.org) [21]
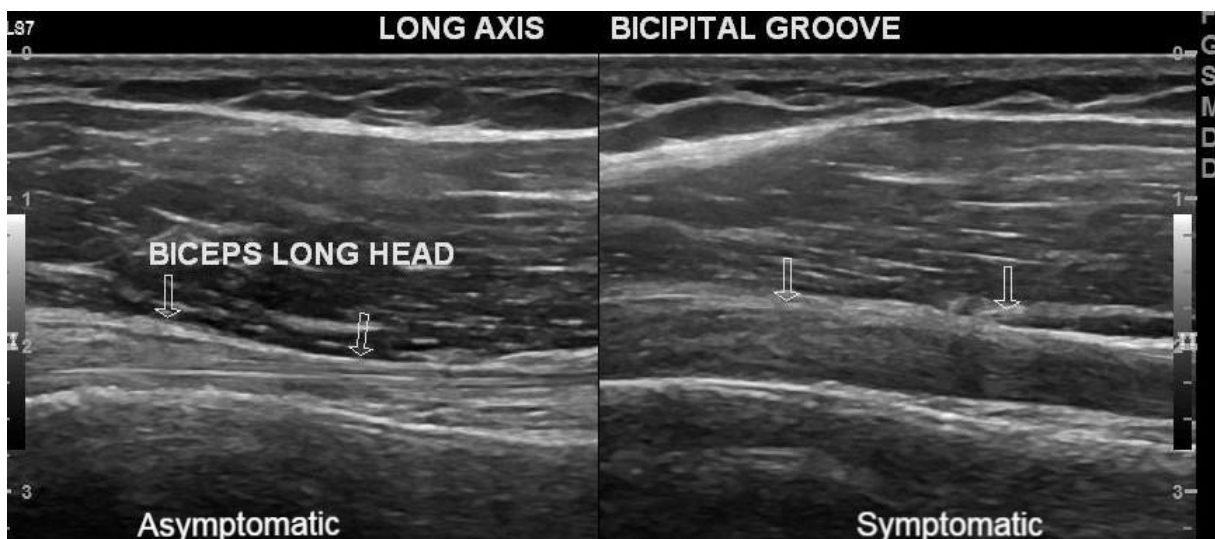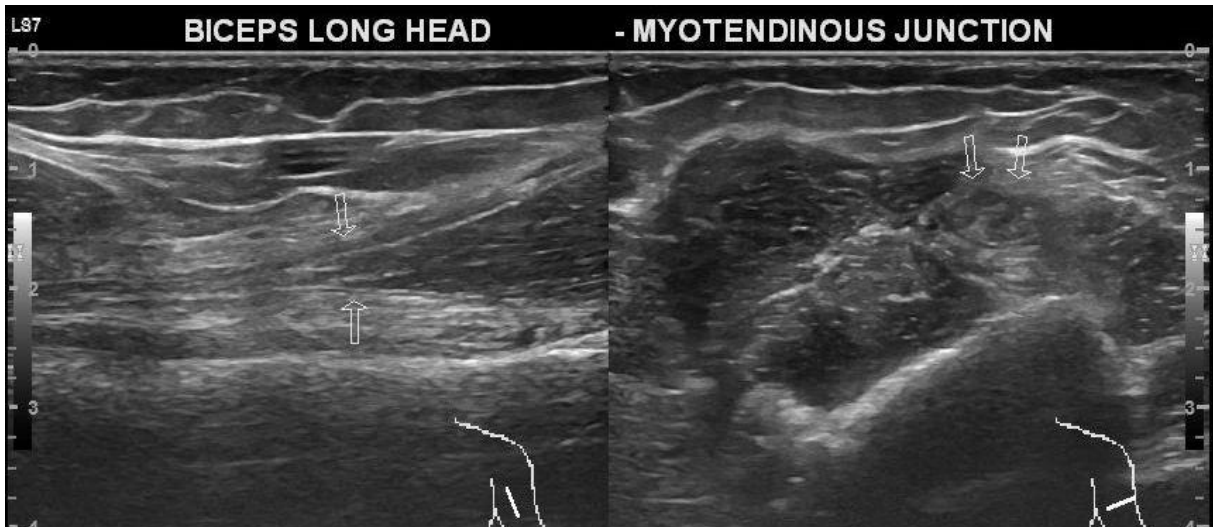
Figure 25: Longitudinal and cross-section of the myotendinous junction of the caput longum of the affected side. (Image source: Stanislavsky A. et al., 2019, radiopaedia.org) [21]

A subpectoral biceps tenodesis was performed for treatment.[21]

5.1.7. Patient case 2: Subdeltoid Lipoma

A 65-year-old man presented with a long-standing mass in his right shoulder. No pain was reported. The clinical examination suggested a lipoma. [22]

The subsequent ultrasound examination showed a sharply defined lesion measuring approx. 70x60x35mm between the humerus and deltoid muscle, which was isoechogenic to the surrounding fatty tissue. No calcifications, cystic changes or hypervascularisation could be detected. The mass could be compressed. The axillary nerve and the accompanying artery were displaced by the lesion. The rotator cuff was intact.[22]
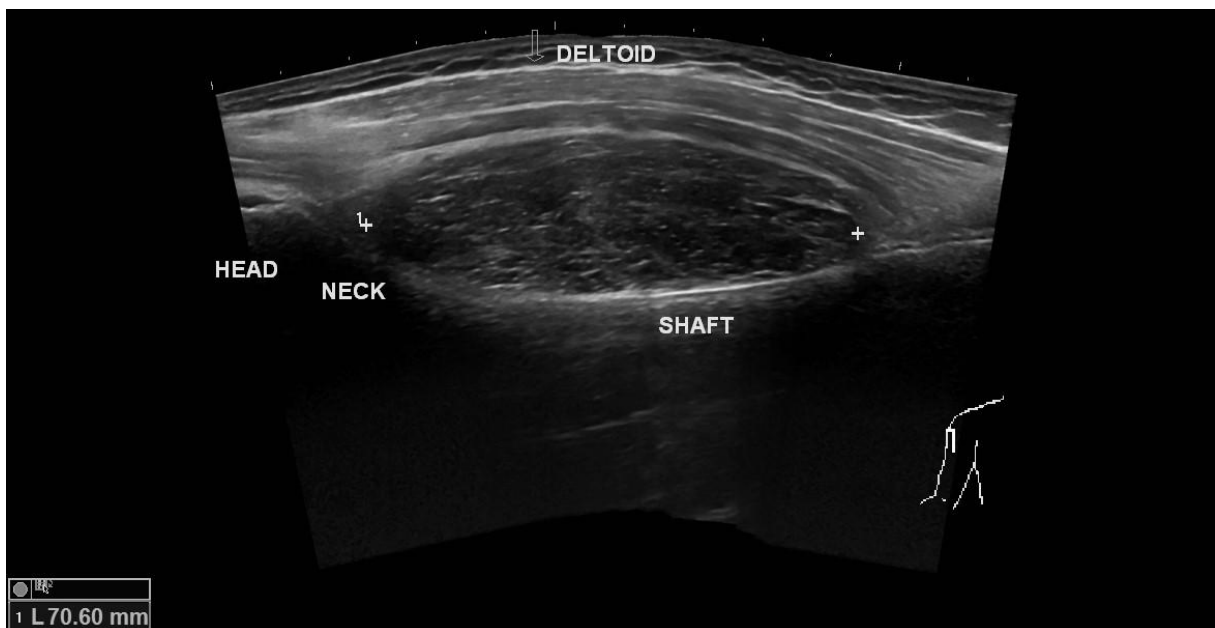

Figure 26: Illustration of the lesion in the coronal section. Panoramic image. (Image sourcce: Patel M., 2019, radiopaedia.org) [22]
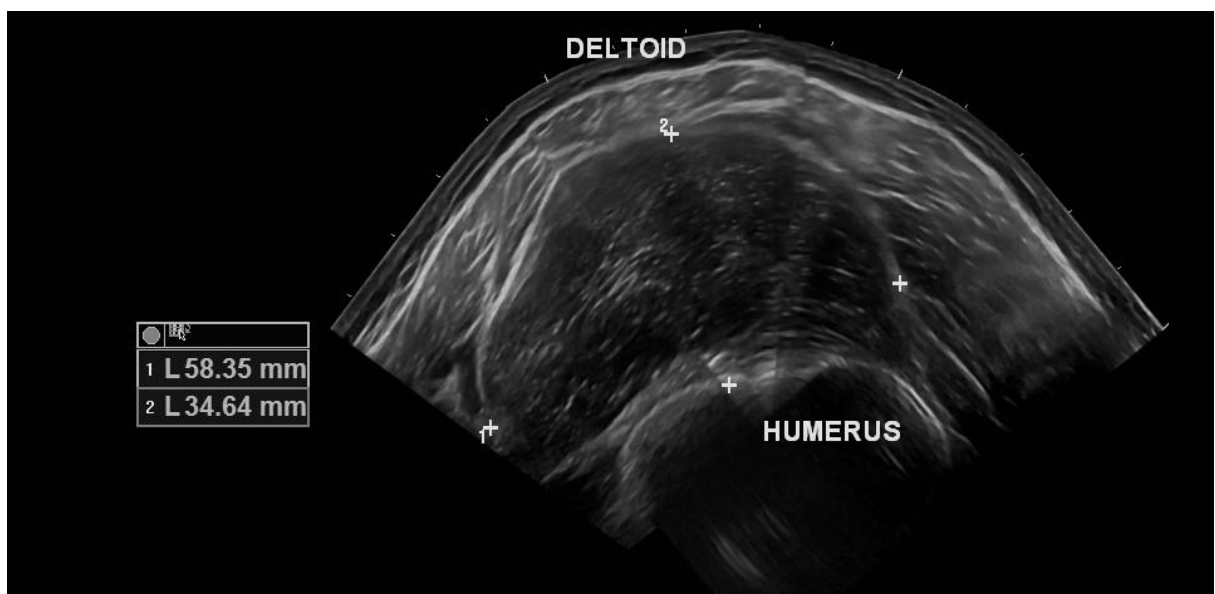
Figure 27: Transverse section of the lesion. Panoramic image. (Image source: Patel M., 2019, radiopaedia.org) [22]

Figure 28: Axillary nerve and artery hit transversely in the coronal section. The displacement of the normally deeper-lying structures can be seen. (Image source: Patel M., 2019, radiopaedia.org) [22]

The ultrasound examination indicated a subdeltoid lipoma with no suspicious signs of liposarcoma. Surgical excision followed. The suspected diagnosis was confirmed.[22]

5.1.8. Patient case 3: Tear of the supraspinatus tendon

A 60-year-old woman presented with pain and abduction weakness in her right shoulder. The symptoms had been present for six months.
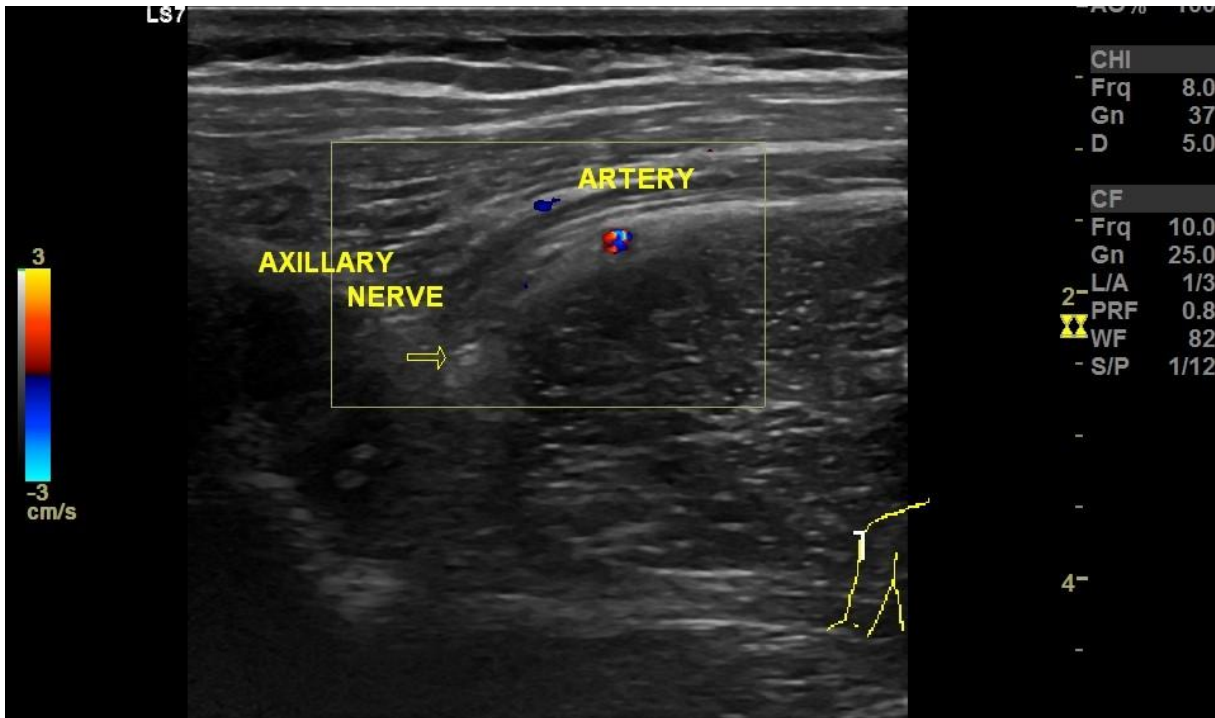
Sonography revealed a fluid-filled defect of approx. 15 mm around the insertion of the right supraspinatus tendon. The subacromial-subdeltoid bursa showed an accumulation of fluid. The rest of the rotator cuff and the opposite side were intact.[23]
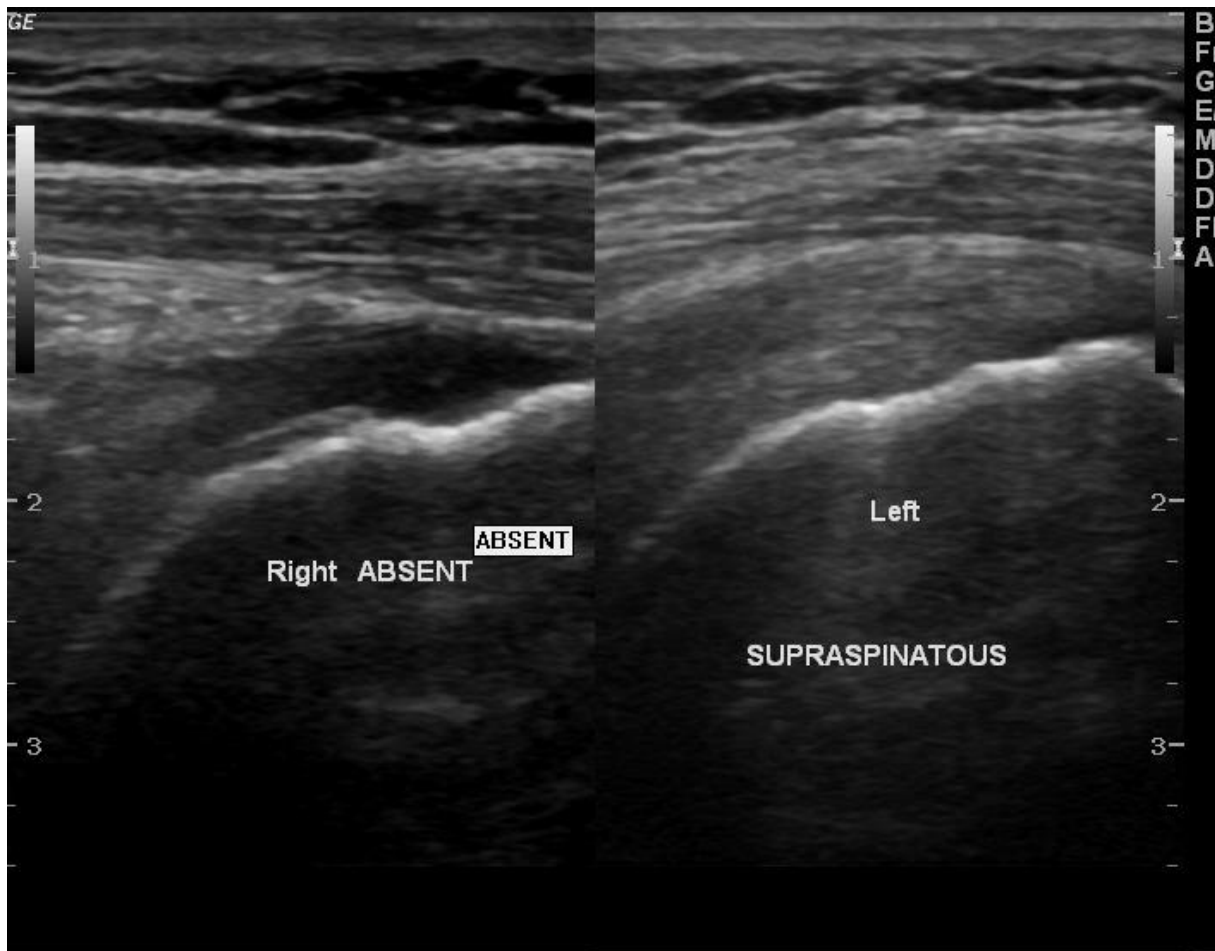

Figure 29: Supraspinatus tendon in longitudinal view: on the left the right, symptomatic shoulder, on the right the left, asymptomatic side (Image source: Jin T. et al., 2010, radiopaedia.org) [23]

The radiological findings suggest a complete rupture of the supraspinatus tendon.[23]

5.2. Elbow

5.2.1. Anterior articular surface

The standardised examination of the elbow is carried out with the elbow joint extended and in the supination position. For patient comfort and to enable full extension, a suitable cushion can be placed under the elbow.[11]
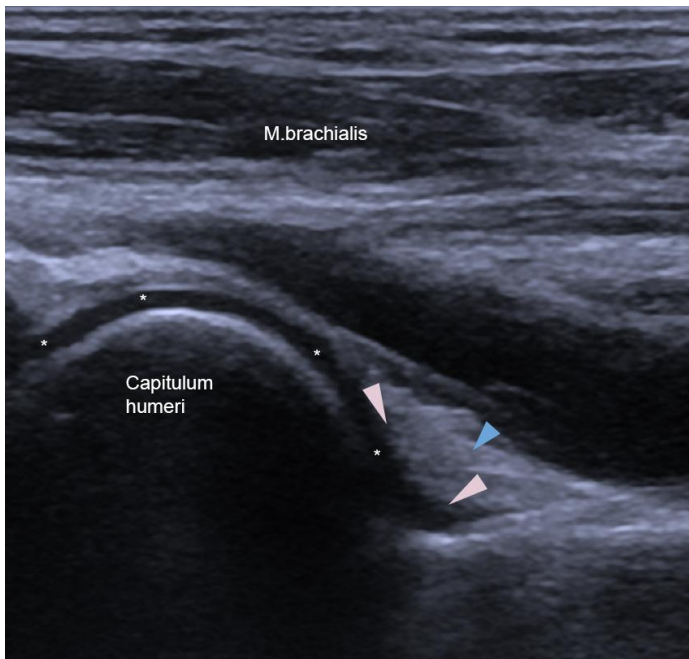
Figure 30: Sagittal section of the anterior elbow joint. Asterisk: Articular cartilage of the distal humeral epiphysis. Blue arrow: Anterior fat pad. Pink arrows: Anterior coronoid recess.

Figure 31: Probe positioning.

Start with the anterior joint surface first. The probe is positioned medially sagittal. By moving the probe laterally, the humeral capitulum (Fig. 30, left, i.e. proximal) is visualised. Distal to this is the anterior fat pad, which fills the coronoid fossa. In a healthy joint, some fluid may be visible between the fat pad and the humerus.[11]
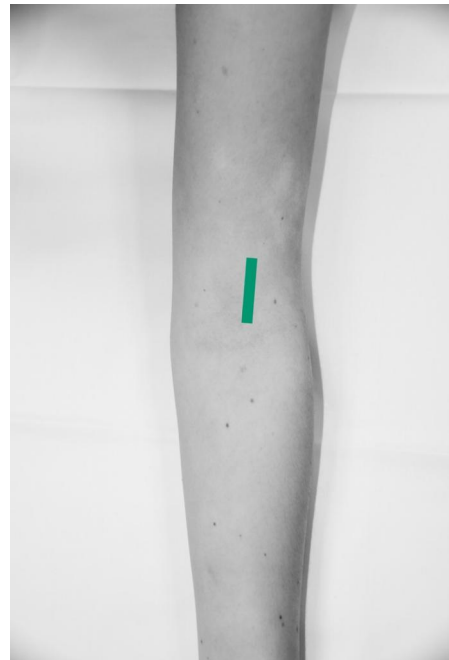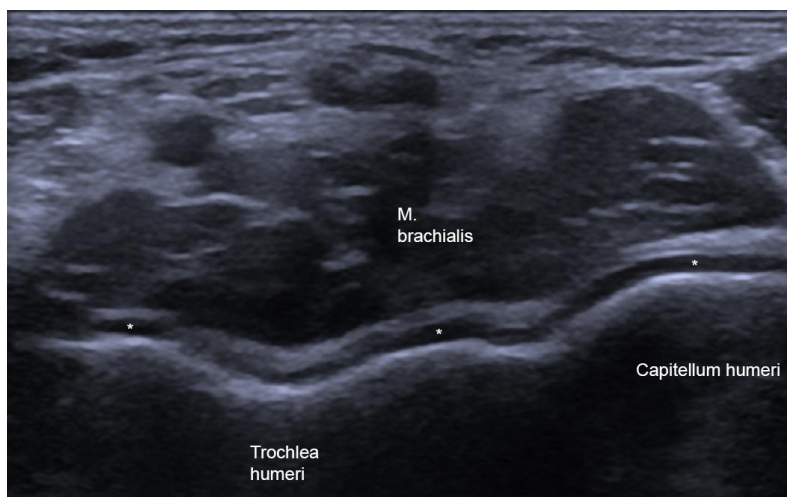
Figure 32: Transverse section of the anterior elbow. Asterisk: Articular cartilage of the distal humeral epiphysis.

Figure 33: Probe positioning.

The distal humeral epiphysis can be seen in the transverse section, covered by a layer of cartilage, which appears undulating here. The humeral capitellum is located laterally and the trochlea medially.[11]

5.2.2. Extensor tendon
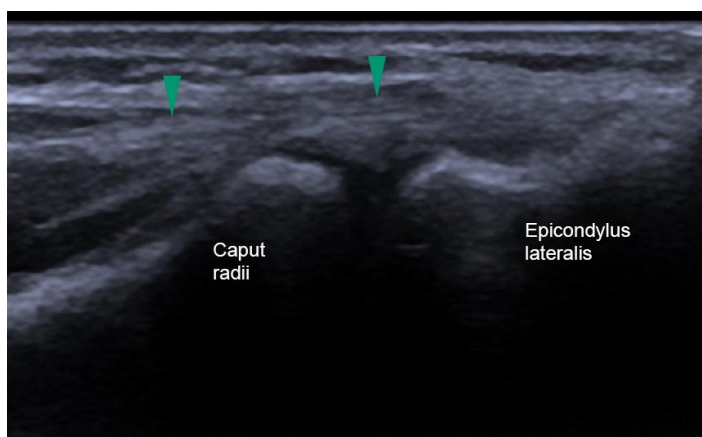
Figure 34: Origin of the extensor muscles in longitudinal view. Green arrows: common extensor tendon.
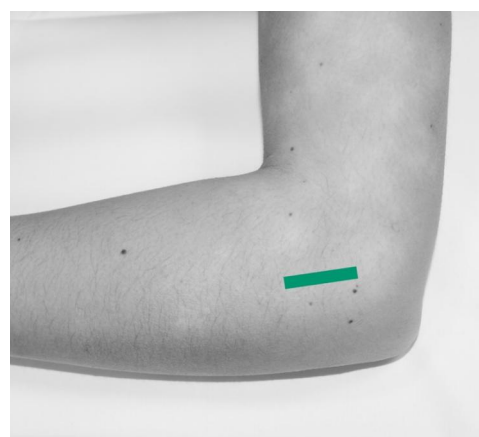
Figure 35: Probe positioning.

To examine the extensor tendon, the elbow is flexed 90° and the forearm is placed on the table in pronation. The probe is placed in the coronal plane, with the proximal end of the probe resting on the lateral epicondyle. In the example shown here for the left arm, the extensor tendon runs from the right in the image (Fig. 34) along the green arrows to the left. It is advisable to also make cross-sections of the tendon. The lateral ulnar collateral ligament cannot normally be delineated.[11]

5.2.3. Radiocapitellar joint
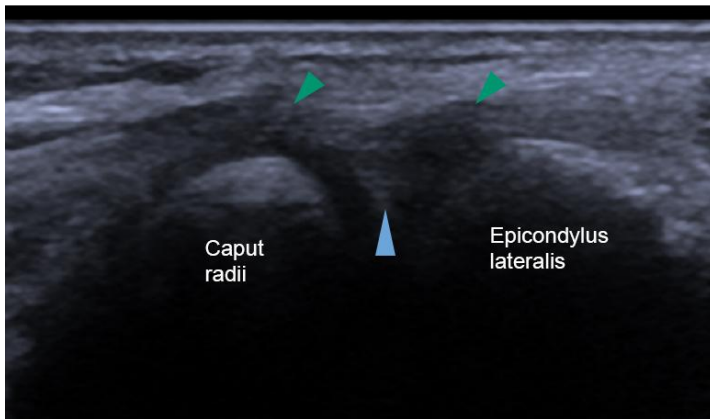
Figure 36: Radiocapitellar joint in longitudinal section. Green arrows: common extensor tendon. Blue arrow: lateral synovial fringe.

Figure 37: Probe positioning.

The radiocapitellar joint can be examined in the same position, although a better image can be achieved if the probe is moved slightly laterally and rotated a few degrees anti-clockwise. The radial head can be dynamically examined by passive pro- and supination, whereby occult fractures can be visualised. The anular ligament should also be examined. The anular recess is only visible if it is dilated with fluid.[11]

5.2.4. Flexor tendon / medial collateral ligament
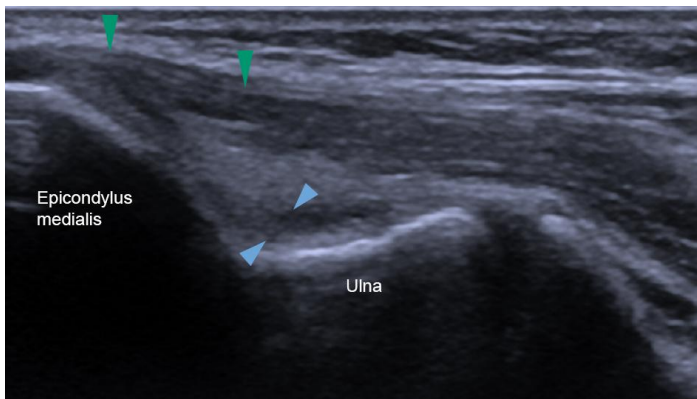
Figure 38: Longitudinal view of the origin of the flexor tendon. Green arrows: Origin of the common flexor tendon. Blue arrows: anterior portion of the medial collateral ligament.
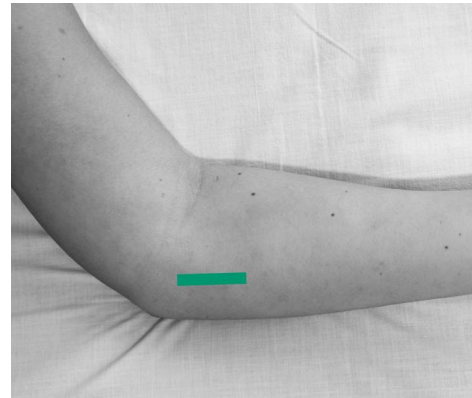
Figure 39: Probe positioning.

To examine the flexor tendon, the patient must lean their upper body towards the side to be examined. The elbow is held almost extended and the forearm in forced supination. The probe is placed with the cranial side on the medial epicondyle (Fig. 39). In this way, a longitudinal section of the flexor tendon is generated, which is thicker and shorter than the extensor tendon. Posterior to the flexor tendon, the anterior part of the medial collateral ligament is visible.[11]

Note: If a partial rupture of the medial collateral ligament is suspected, the arm can be examined in an extended position under valgus stress (preferably with an assistant). In the case of partial tears, the joint space can be widened under load, but not in a healthy joint.[11]

5.2.5. Triceps tendon
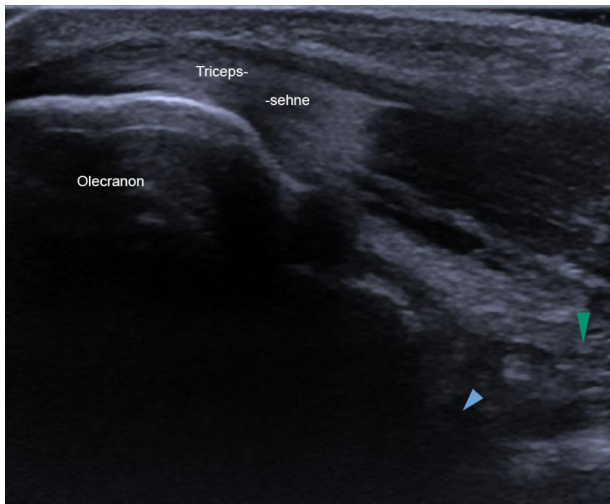
Figure 40: Longitudinal view of the insertion of the triceps tendon. Green arrow: posterior fat pad. Blue arrow: posterior olecranon recess.

Figure 41: Probe positioning.

To examine the triceps tendon, the elbow is flexed 90° with the palm of the hand resting on the examination table. The probe is positioned in the longitudinal axis directly proximal to the olecranon in order to assess the insertion of the triceps tendon. Particular attention must be paid to the distal part of the triceps tendon in order to rule out enthesitis.[11]

The posterior olecranon recess is located anterior to the tendon. A suspected joint effusion can be visualised or excluded here by examining the joint at 45° flexion. This shifts any small effusion from the anterior part of the joint to the posterior. Slight shaking movements of the elbow can help to move the fluid. It is particularly important not to apply great pressure to the probe so as not to push away any effusions.[11]

5.2.6. Patient case 4: Triceps tendon rupture

A 35-year-old man presented after sustaining an elbow injury while weightlifting. X-rays taken in two planes showed no evidence of fresh osseous lesions. In the subsequent ultrasound examination, the triceps tendon on the symptomatic side was found to be 18 mm retracted and coiled. A narrow anechoic rim around the tendon is most likely consistent with a resulting haematoma. The opposite side showed normal echo structure and anatomy of the triceps tendon. The findings are in favour of a high-grade triceps tendon rupture and avulsion.[24]

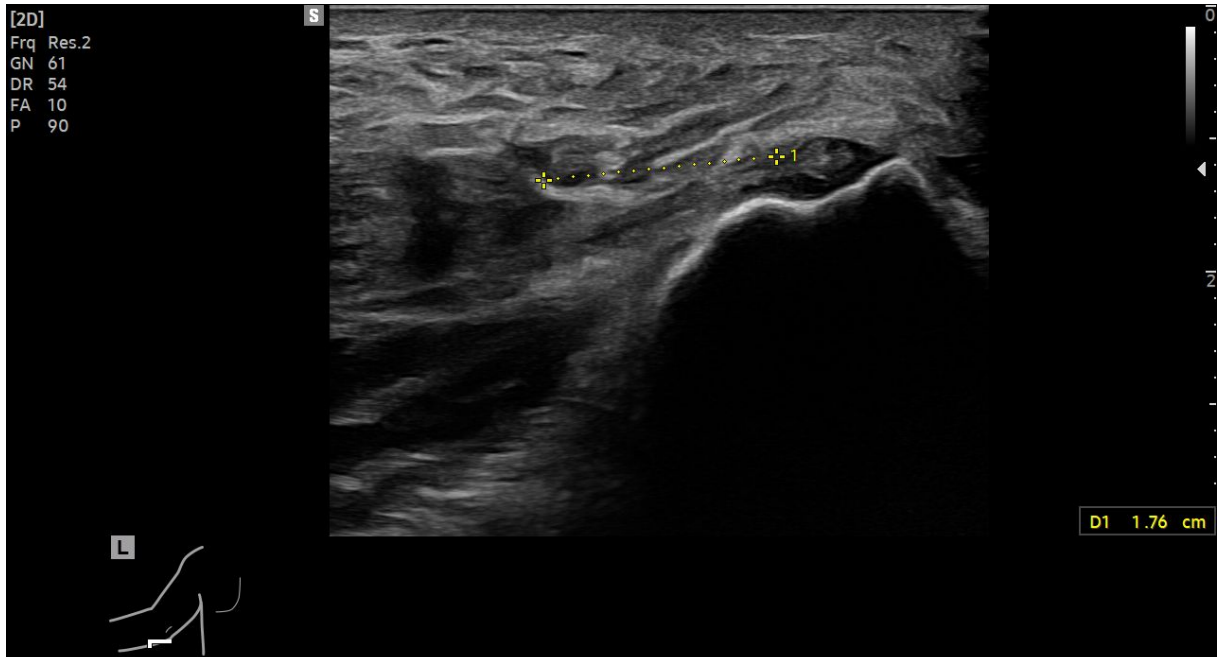*Figure 42: Longitudinal section of the left triceps tendon. Retraction by just under 18mm. (Image source: Botz B., 2022, radiopaedia.org)* [24]
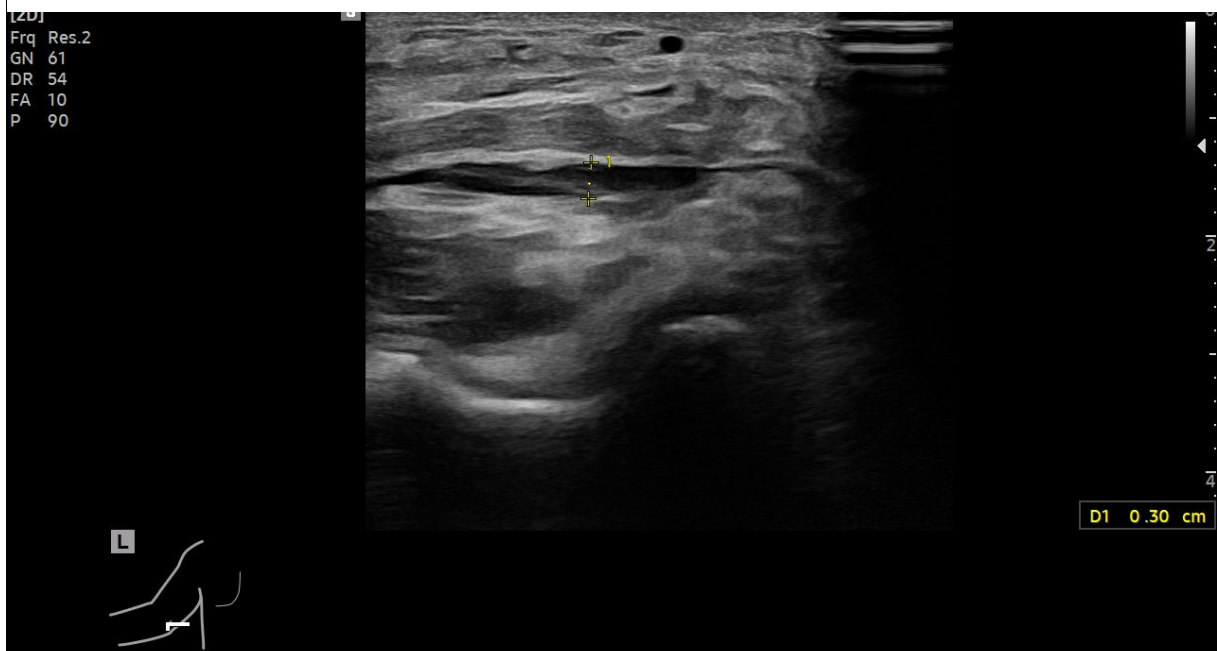

Figure 43: Longitudinal section of the left triceps tendon. Narrow anechoic rim, compatible with a haematoma. (Image source: Botz B., 2022, radiopaedia.org) [24]
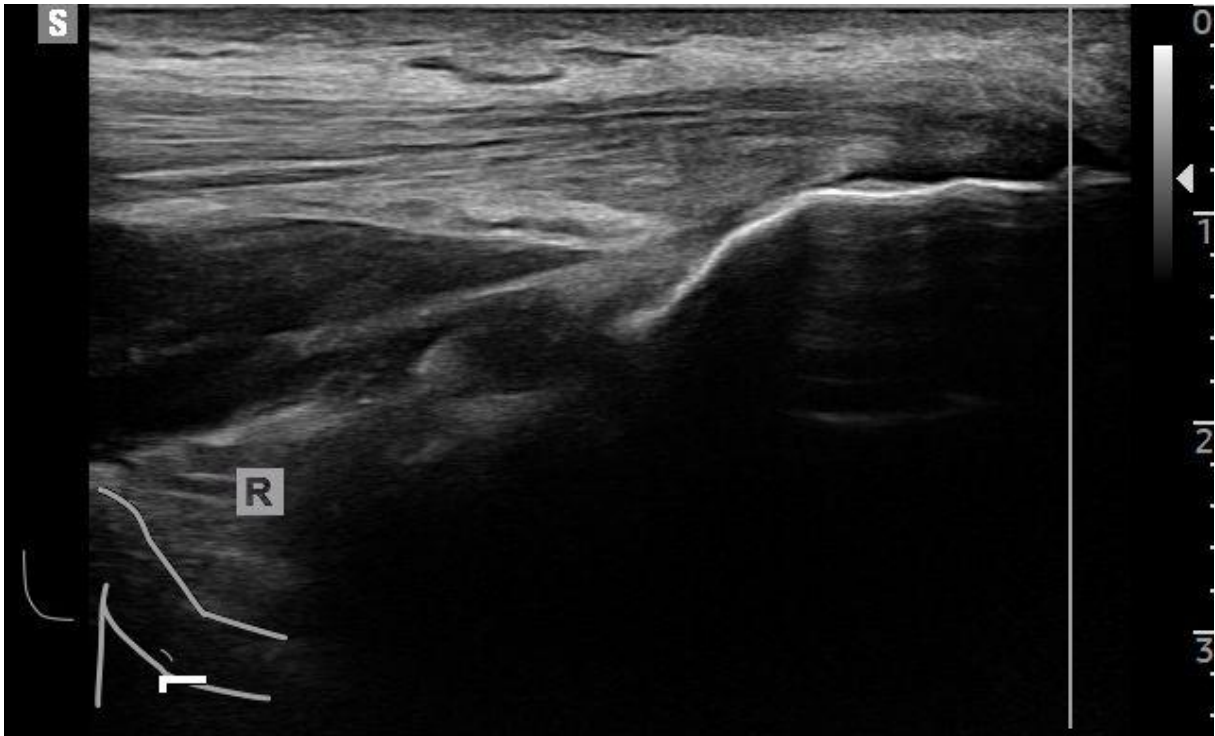
Figure 44: Opposite side in the same section for comparison. (Image source: Botz B., 2022, radiopaedia.org) [24]

5.2.7. Patient case 5: bilateral anconeus epitrochlearis muscle

A 30-year-old male presented with right shoulder pain with stiffness in the elbow over the last few months. The subsequent ultrasound examination revealed an additional structure superficial to the ulnar nerve, which continued from the medial epicondyle to the ulnar olecranon process and showed a muscular echo pattern. Flexion in the elbow resulted in compression of the ulnar nerve between the superficial accessory muscle and the deeper ulnar collateral ligament. The additional muscle could be visualised on both sides. It is the anconeus epitrochlearis muscle on both sides, an accessory muscle of the medial elbow. The differential diagnosis excluded oedema of the ulnar nerve and carpal tunnel syndrome.[25]

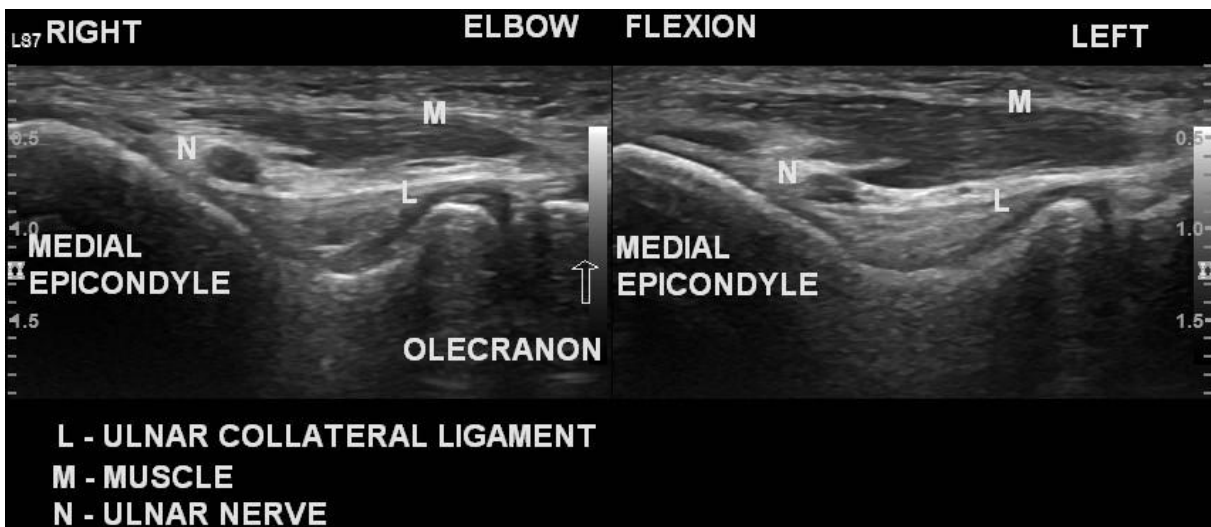*Figure 45: Longitudinal section of the muscle. Both extremities shown. (Image source: Patel M., 2020, radiopaedia.org)* [25]
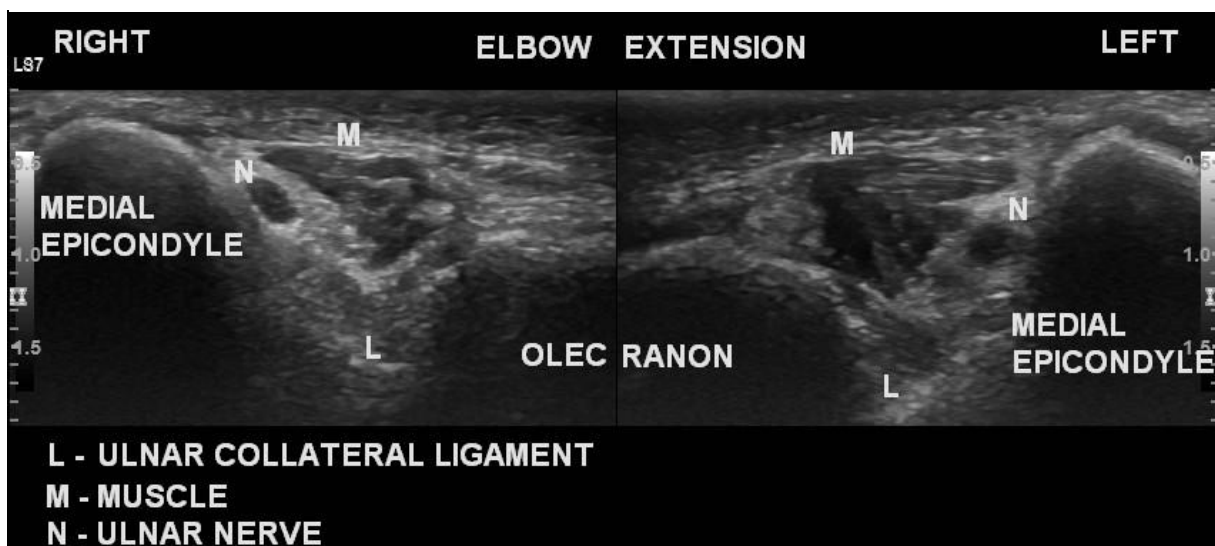

Figure 46: Cross-section of the muscle. Both extremities shown. (Image source: Patel M., 2020, radiopaedia.org) [25]

5.2.8. Patient case 6: Medial elbow snapping

A 15-year-old girl presented with numbness and tingling in the fourth and fifth fingers on the right. The symptoms had been present for the last few days. She was not aware of any trauma. Sonography revealed a normal position in extension and slight oedema of the ulnar nerve (Fig. 47). Under 90° flexion in the elbow joint, the ulnar nerve dislocated anterior to the medial epicondyle (Fig. 48). Under complete flexion, the caput mediale of the triceps also dislocated (Fig. 49). Under extension, the muscle dislocated first, followed by the nerve.[26]

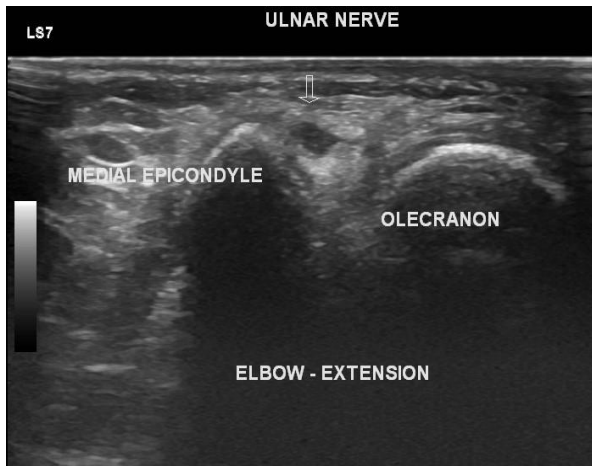*Figure 47: Normal anatomy under extension except for slight oedema of the ulnar nerve. Graphic cropped. (Image source: Patel M., 2023, radiopaedia.org)* [26]
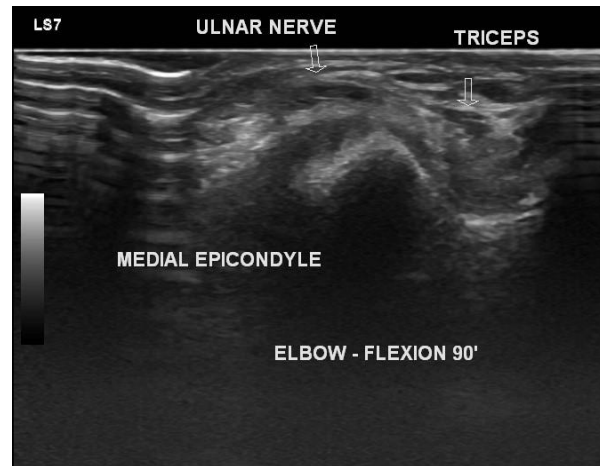
Figure 48: Dislocation of the ulnar nerve at 90° flexion. (Image source: Patel M., 2023, radiopaedia.org) [26]
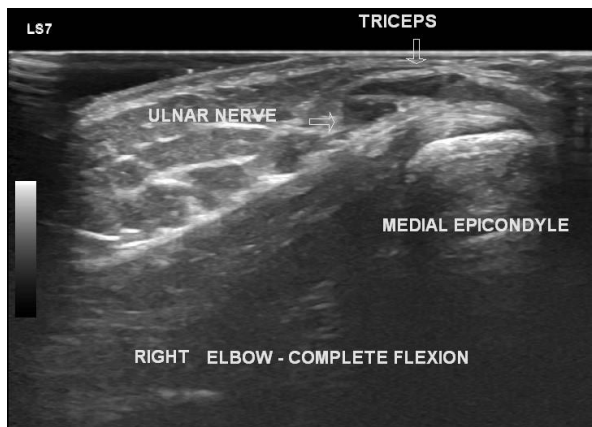
Figure 49: Dislocation of the triceps muscle, caput mediale in complete flexion. (Image source: Patel M., 2023, radiopaedia.org) [26]

5.3. Wrist

5.3.1. Compartment I
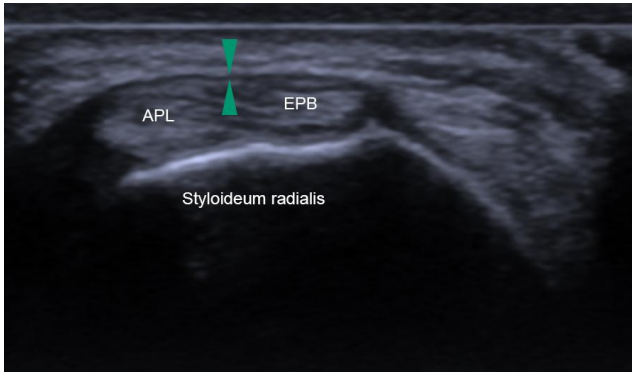
Figure 50: Cross-stection of the Compartment I. APL : M.abductor pollicis longus. EPB : M.extensor pollicis brevis. Arrows : Retinaculum.

Figure 51: Probe positioning.

The examination of the wrist begins with the examination of Compartment I. To do this, the patient is asked to hold the forearm in a neutral position. The probe is placed transversely on the radial styloid. The tendons of the abductor pollicis longus (ventrally located) and the extensor pollicis brevis (dorsally located) can be examined here. Particular attention should be paid to the question of whether the retinaculum is intact and whether there is a vertical septum. Possible additional tendons can be detected in the distal course of the tendons.[27]

5.3.2. Compartment II
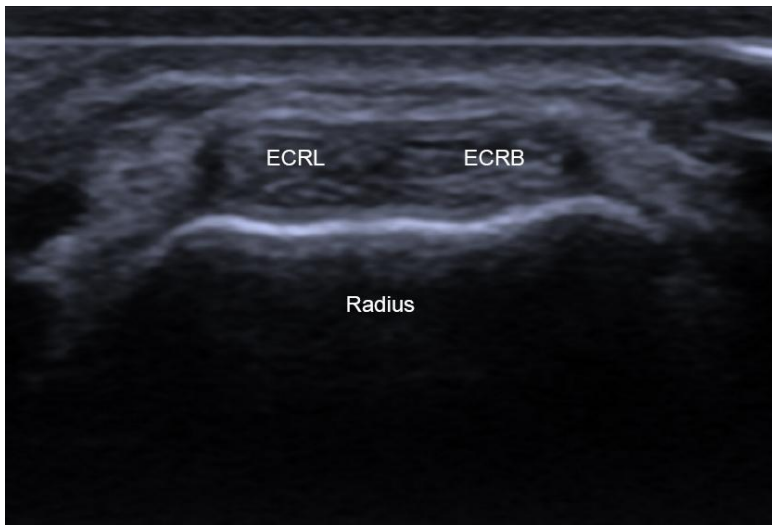
Figure 52: Cross-section of Compartment II. ECRL: M.extensor carpi radialis longus. ECRB: M.extensor carpi radialis brevis.
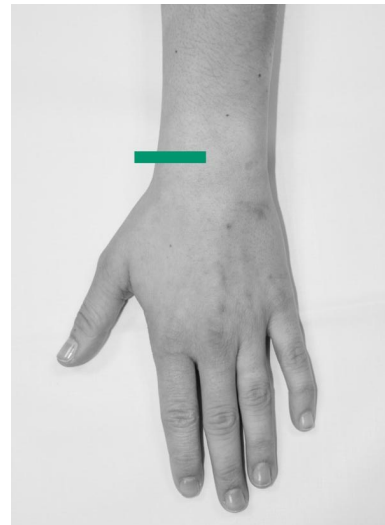
Figure 53: Probe positioning.

To examine compartment II, the forearm is brought into a pronated position so that the palm of the hand rests on the examination table. The probe is moved ulnarly from the previous position in order to visualise the second compartment, which contains the tendons of the extensor carpi radialis brevis and longus muscles. If the probe is moved proximally (Fig. 54, 55), the crossing of the tendons of the first compartment can be visualised.[27]

Figure 54: Cross-section of Compartment II, more proximal. Arrows: Muscles of compartment I crossing the ECRL and ECRB.
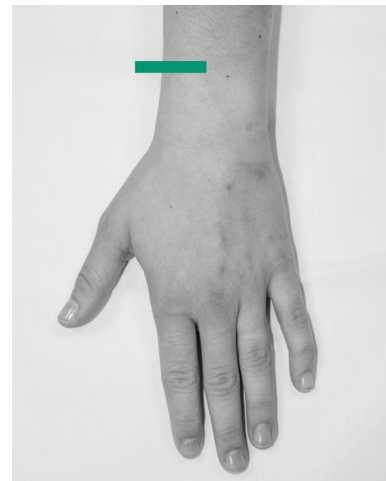
Figure 55: Probe positioning. Note the proximal shift.

5.3.3. Compartment III/IV/V

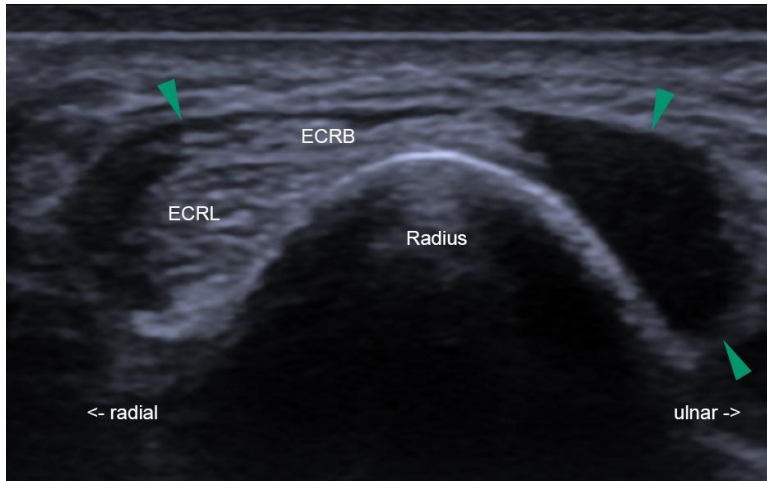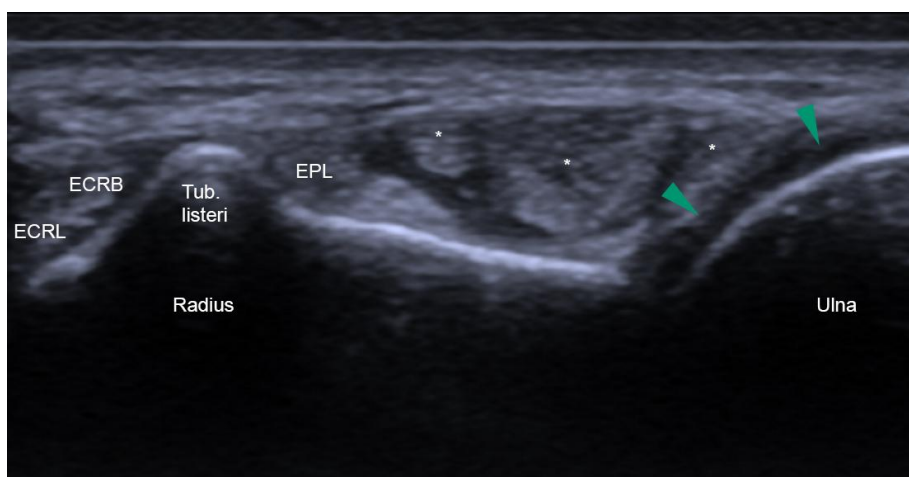*Figure 56: Cross-section of Compartment III/IV/V. EPL: M.extensor pollicis longus. Asterisk: M.extensor digitorum communis. Arrows: Articular cartilage of the ulnar capitulum.*

Figure 57: Probe positioning.

The patient positioning from before is maintained. The probe is moved further ulnarly to examine compartments III (extensor pollicis longus), IV (extensor digitorum communis, extensor indicis proprius) and V (extensor digiti minimi). To differentiate between the tendons in compartment IV and to recognise the extensor digiti minimi, it may be helpful to ask the patient to flex/extend individual fingers. A low-echo rim can be seen dorsally of the ulna, which is caused by the articular cartilage of the ulnar capitulum. It should not be confused with effusion.[27]

5.3.4. Compartment VI
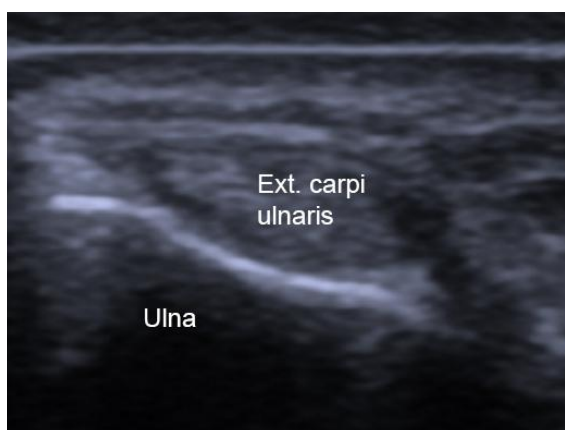
Figure 58: Cross-section of the Compartment VI.
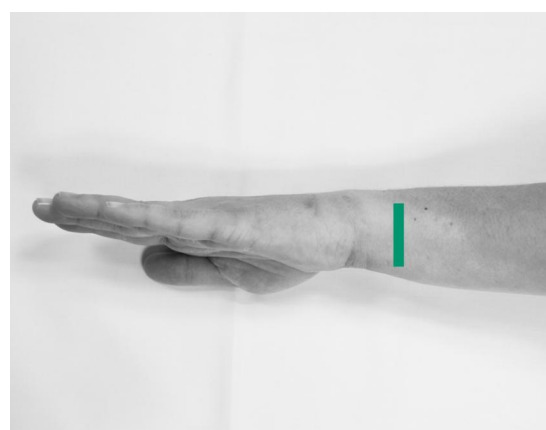
Figure 59: Probe positioning.

To examine compartment VI, the forearm is positioned in an over-rotated pronated position with the radius side in contact with the table surface. The probe is placed on the ulna directly proximal to the transverse ulnar styloid process in order to examine the tendon of the extensor carpi ulnaris muscle.[27]

5.3.5. Radiocarpal and midcarpal joints
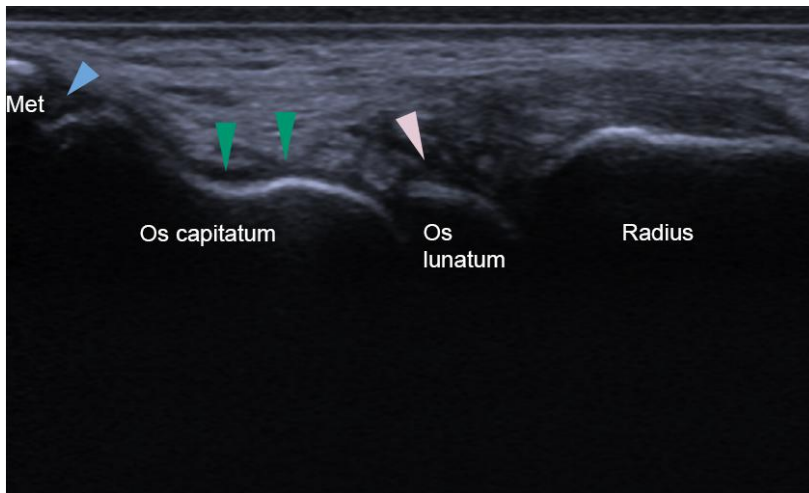
Figure 60: Longitudinal view of the radiocarpal and midcarpal joints. Met: Os metacarpale. Green arrows: dorsal recess of the midcarpal joint. Blue arrow: dorsal recess of the carpometacarpal joints. Pink arrow: dorsal recess of the radiocarpal joint.
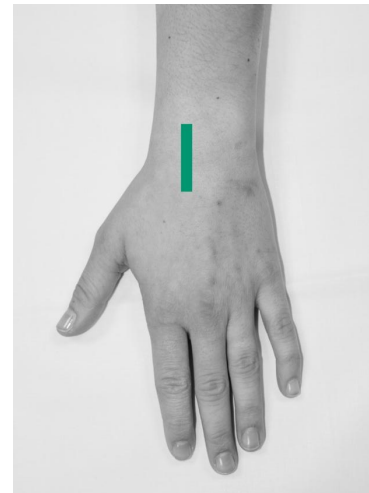
Figure 61: Probe positioning.

To examine the radiocarpal and midcarpal joints, the forearm is returned to the pronated position so that the palm rests on the table. The ultrasound probe is positioned longitudinally. The synovial recess of the radiocarpal and midcarpal joints can be examined in this way. Particular attention should be paid to effusion or synovial thickening. Dorsally, the extensor tendons run longitudinally in the image (Fig. 60, in the image above) [27]

5.3.6. Carpal tunnel
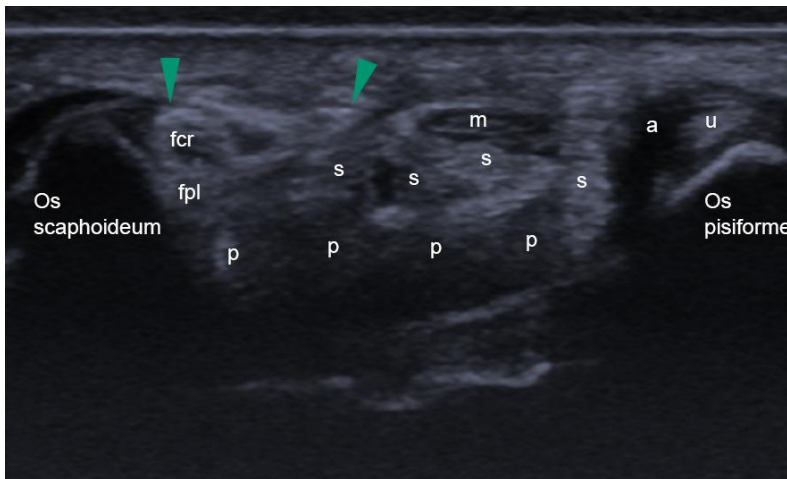
Figure 62: Carpal tunnel in cross-section. fcr: M.flexor carpi radialis. fpl: M.flexor pollicis longus (tendon). s: M.flexor digitorum superficialis (tendon). p: M.flexor digitorum profundus (tendons). a: A.ulnaris. u: ulnar nerve. m: median nerve. Green arrows: Retinaculum flexorum.

Figure 63: Probe positioning.

To examine the carpal tunnel, the forearm is placed in a supinated position so that the back of the hand touches the table surface. The probe is placed transversely at the level of the proximal carpal tunnel so that the scaphoid tubercle is visible on the radial side and the pisiform bone on the ulnar side. Slight tilting can help to visualise the soft structures. In particular, the flexor retinaculum (Fig. 62, green arrows) should be checked, as well as all nine long flexor tendons (flexor digitalis superficialis: four tendons, flexor digitalis profundus: four tendons, and flexor pollicis longus). If there is a clinical suspicion of a tendon lesion, the integrity can be checked in the longitudinal axis with passive movement. Attention should also be paid to any muscle malformations or tendosynovitis. The tendon of the flexor carpi radialis muscle should be checked on the radial side.[27]

5.3.7. Patient case 7: Flexor pollicis longus

A 20-year-old male presented for a sonographic examination. One month previously, he had sustained a cut to his right wrist. Clinical findings included a loss of flexion in interphalangeal joint I and reduced sensitivity in the radial fingers. Sonography revealed a laceration of the flexor pollicis longus muscle, which widened to approx. 25 mm when flexion was attempted, suggesting that it had been completely severed. The median nerve also showed a laceration of approx. 5mm. Both findings could explain the patient's symptoms. The diagnosis was confirmed intraoperatively.[28]
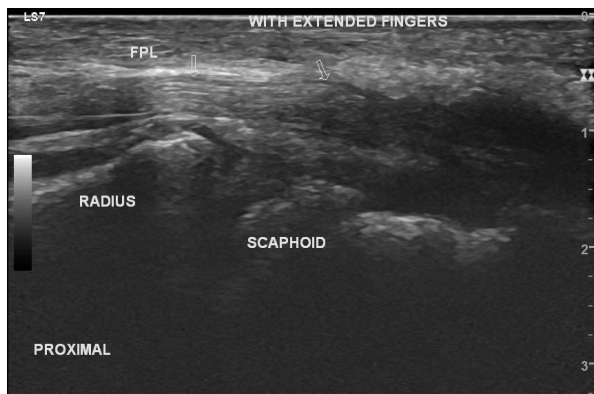
Figure 64: Longitudinal view of the tendon of the flexor pollicis longus with the finger extended. (Image source: Patel M., 2021, radiopaedia.org) [28]
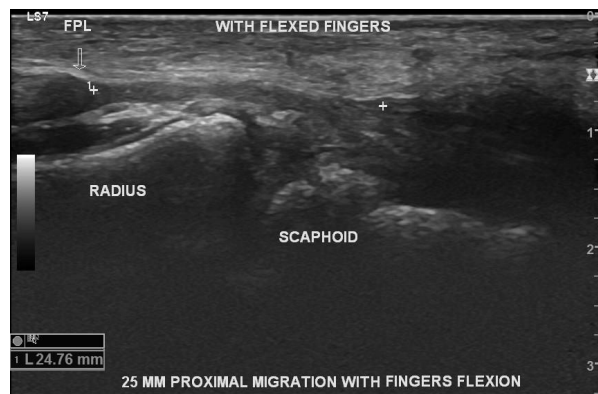
Figure 65: Longitudinal view of the flexor pollicis longus tendon during attempted flexion. (Image source: Patel M., 2021, radiopaedia.org) [28]
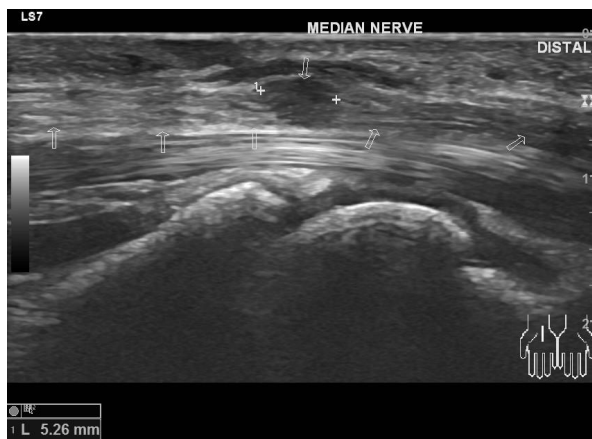
Figure 66: Longitudinal view of the median nerve (arrows) with laceration of approx. 5mm. (Image source: Patel M., 2021, radiopaedia.org) [28]

5.3.8. Patient case 8: Carpal tunnel syndrome

A 70-year-old man was referred for an ultrasound examination with suspected left carpal tunnel syndrome. Sonography revealed oedema of the median nerve directly proximal to the left carpal tunnel. The diameter of the nerve was approx. 14 mm^2. The nerve was compressed in the carpal tunnel (Fig. 68). No mass was seen in the tunnel, nor was there a bifid median nerve or persistent median artery.[29]

Figure 67: Cross-section of the left median nerve. Graphic cropped. (Image source: Patel M., 2018, radiopaedia.org) [29]
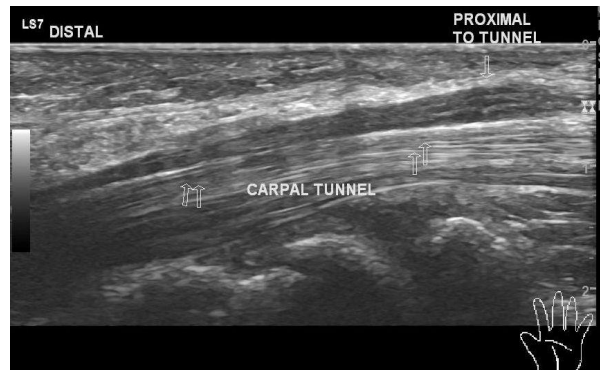
Figure 68: Longitudinal view of the left median nerve with visible compression in the carpal tunnel. (Image source: Patel M., 2018, radiopaedia.org) [29]

5.3.9. Patient case 9: Ganglion of the scaphotrapezial joint

A 20-year-old woman presented with a palmar-radial lump of the left wrist. She reported moderate pain over the last few months.[30]

Sonography revealed a well-defined, lobulated, thin-walled, anechoic avascular lesion (approx. 13x7x2mm) in the region of the scaphotrapezial joint. A small incomplete septum was recognisable as well as a dorsal sound enhancement. The pedicle process of the lesion extended to the scaphotrapezial joint. The nearby tendon of the flexor carpi radialis muscle was normal.[30]

Figure 69: Longitudinal view of the lesion. FCR: Flexor carpi radialis. (Image source: Patel M., 2021, radiopaedia.org) [30]
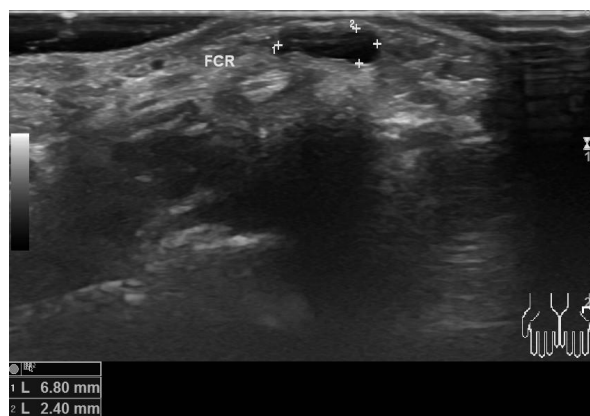
Figure 70: Cross-section of the lesion (Image source: Patel M., 2021, radiopaedia.org) [30]

The case shows a volar ganglion of the wrist, originating from the scaphotrapezial joint. A ganglion is the most common mass lesion in the hand and wrist.[30]

5.4. Hip

5.4.1. anterior joint surface / iliopsoas tendon
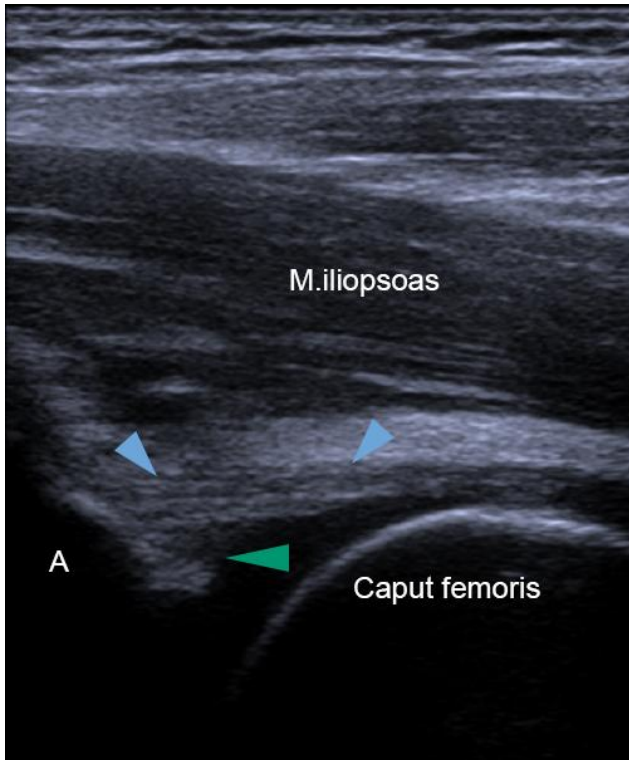
Figure 71: sagittal view of the anterior hip joint. A: Acetabulum. Green arrow: glenoid. Blue arrows: Lig.iliofemorale.

Figure 72: Probe positioning.

To examine the hip, the patient is placed in the supine position. To assess the iliopsoas tendon and anterior joint capsule, the probe is positioned in the sagittal plane at the level of the femoral head. The glenoid appears here proximal to the joint capsule as a hyperechoic triangle, similar to the structure of the meniscus of the knee. Additionally, the iliofemoral ligament can be assessed in this position as well if desired.[31]

In obese patients, it can be helpful to switch to a convex probe with a lower frequency in order to adequately visualise the deep-seated structures. [31]

5.4.2. M.tensor fasciae latae / M.sartorius
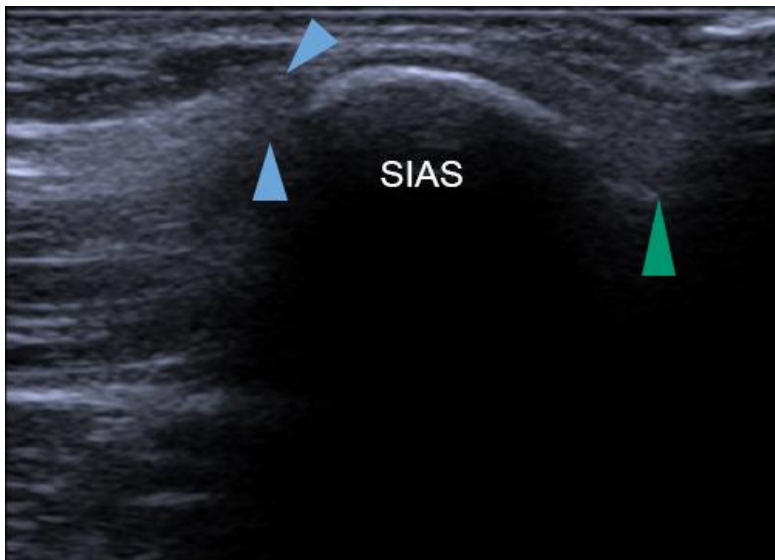
Figure 73: Transverse view. Green arrow: M.tensor fasciae latae. Blue arrow: M.sartorius.
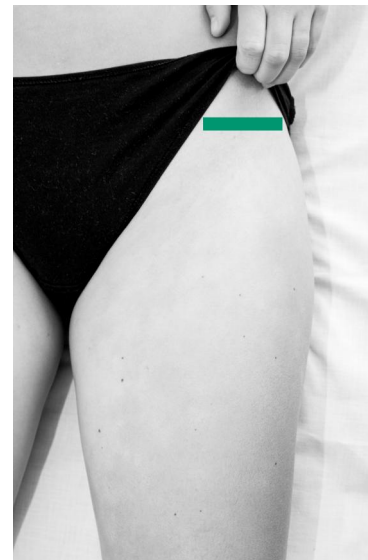
Figure 74: Probe positioning.

To examine the origins of the Mm.tensor fasciae latae et sartorius, the probe is positioned in the transverse plane at the level of the anterior superior iliac spine. The image shows the short tendon origins lateral (M.tensor fasciae latae, blue arrows) and medial (M.sartorius, green arrow) of the hyperechogenic line of the anterior superior iliac spine.[31]
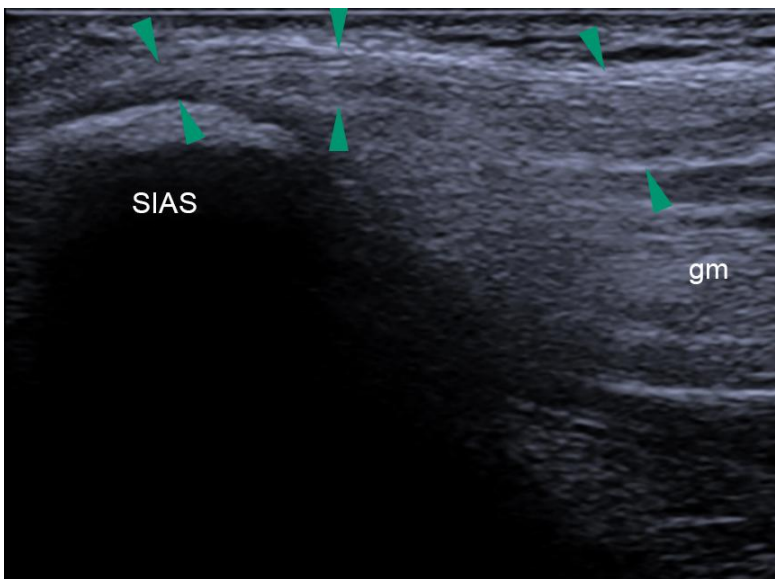
Figure 75: Sagittal view. SIAS: Spina iliaca anterior superior. gm: M.gluteus medius. Green arrows: M.tensor fasciae latae.

Figure 76: Probe positioning.

The muscles can be visualised and traced in longitudinal section by rotating them through 90°. The tensor fasciae latae muscle (Fig. 75, green arrows) is shown here, which can be traced by moving it caudally to the insertion on the iliotibial tract.[31]

5.4.3. Adductor muscles
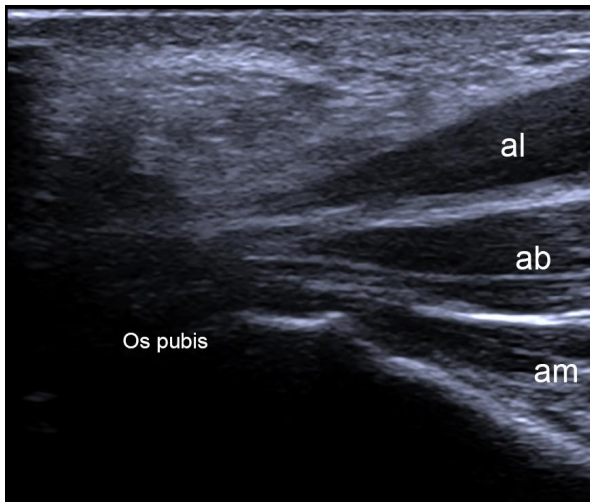
Figure 77: Longitudinal view of the origin of the adductors. al: M.adductor longus. ab: M.adductor brevis. am: M.adductor magnus.

Figure 78: Probe positioning on the protruding adductor muscles.

To examine the medial hip, the hip is abducted and externally rotated and the knee is flexed. The probe is placed on the protruding adductors in the longitudinal axis of the leg. The protruding os pubis can be used as a landmark for the proximal end of the probe. Three muscle layers can be seen, from superficial to deep: [31]

1. M.adductor longus (al)
2. M.adductor brevis (ab)
3. M.adductor magnus (am)

5.4.4. M.gluteus minimus/medius, fascia lata
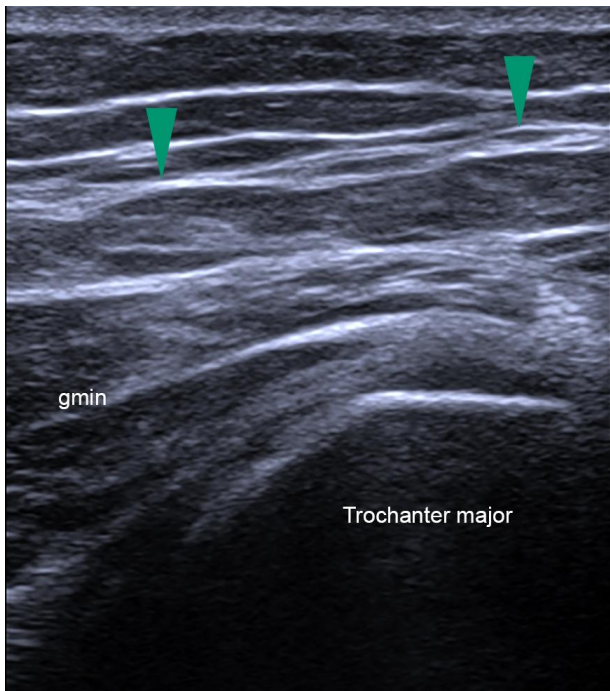
Figure 79: Coronal view. gmin: M.gluteus minimus.
Green arrows: Fascia lata.

Figure 80: Probe positioning.

To examine the lateral hip, the patient is asked to lie on the contralateral side. The probe is placed in the coronal section at the level of the greater trochanter and moved slightly proximally so that it is at the distal edge of the image. The distal part of the gluteus minimus muscle and its insertion can be examined here, as can the tendon of the tensor fasciae latae muscle and the transition into the iliotibial tract.[31]

Figure 81: Cross section. Blue arrow: tendon of the M.gluteus minimus. Pink arrow: M.gluteus maximus.

Figure 82: Probe positioning.

In cross-section, the greater trochanter is also visible as an echoic line in depth. The insertion of the gluteus minimus muscle (Fig. 81, blue arrow) is located anteriorly. By moving it posteriorly, the gluteus maximus muscle can be examined first and the gluteus medius muscle (not shown here) further posteriorly. In a healthy patient, the bursae around the greater trochanter are not visible.[31]

5.4.5. Hamstrings
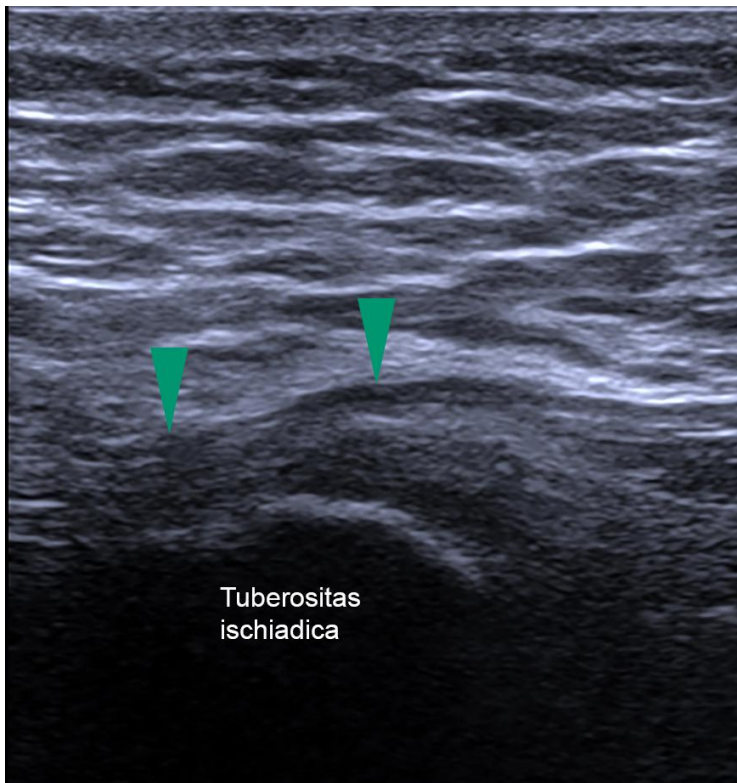
Figure 83: Sagittal view. Green arrows: common tendon insertion of the hamstrings.
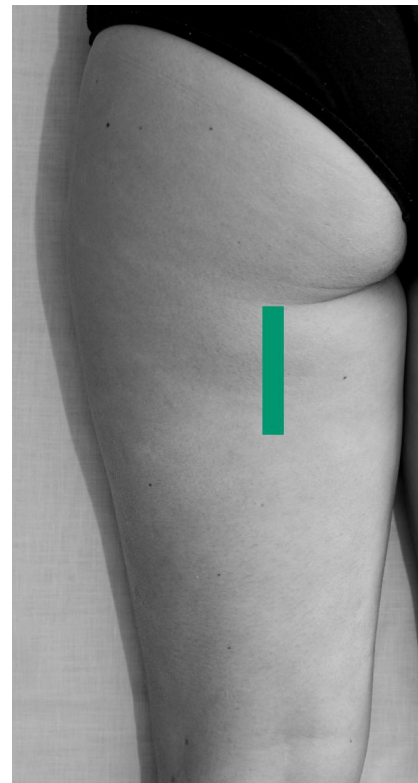
Figure 84: Probe positioning.

To examine the posterior aspects of the hip, the patient is placed in the prone position. The probe is positioned sagittally in order to locate the ischial tuberosity. Directly proximal to this, the common tendinous origin (Fig. 83, green arrows) of the following muscles can be visualised: Mm.semimembranosus, semitendinosus et biceps femoris, caput longum. The individual tendons cannot usually be differentiated using the examination technique shown here.[31]

5.4.6. Herniae

The patient is placed in the supine position to clarify whether an inguinal hernia is present. The probe is placed transversely over the lateral edge of the rectus abdominis muscle (see Figs. 85, 86 and 87). Under Doppler control, the inferior epigastric artery (Fig. 86 and 88: IEA), which originates from the external iliac artery (EIA), can be visualised by moving the probe inferolaterally. The probe is rotated clockwise by approx. 70° in order to visualise the inguinal canal in cross-section (Fig. 89). The entire length can be searched for a hernia by transverse displacement. Rotation by 90° anti-clockwise also visualises the longitudinal section (Fig. 90).[33]
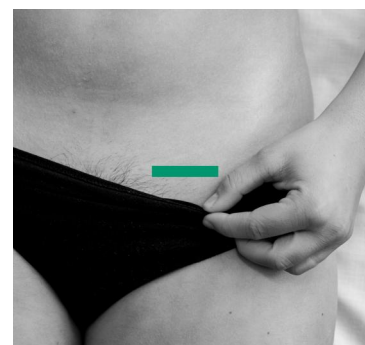
Figure 85: Probe positioning.

A direct inguinal hernia passes through the medial inguinal fossa and exits through the superficial inguinal annulus.[33]

An indirect inguinal hernia, on the other hand, penetrates through the profundus inguinalis annulus, runs in the inguinal canal and exits through the superficial inguinalis annulus. In both cases, a passage can be provoked by increasing the pressure in the abdominal cavity (e.g. Valsalva manoeuvre or coughing).[33]
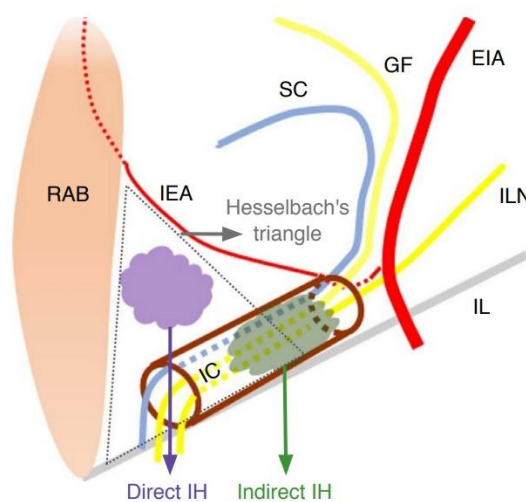
Figure 86: Anatomy of the inguinal canal. RAB: M.rectus abdominis. IEA: A.epigastrica inferior. SC: spermatic cord. GF: N.genitofemoralis, ramus genitalis. EIA: A.iliaca externa. ILN: N.ilioinguinalis. IL: Lig.inguinale. IC: Inguinal canal. (Image source: Wu WT et al., Ultrasonography 2022) [33]
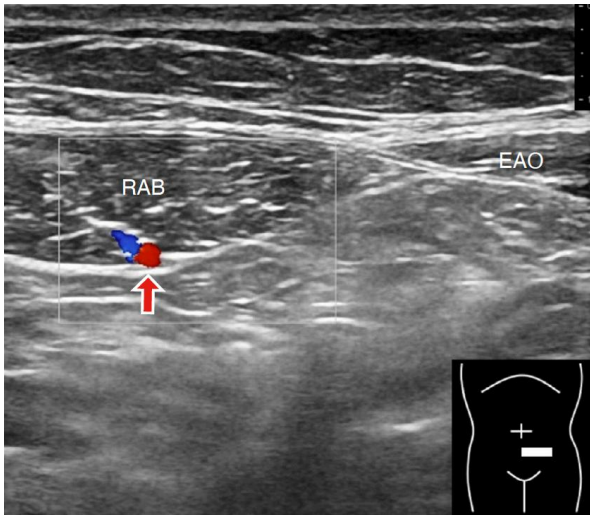
Figure 87: Lateral transverse section of the rectus abdominis muscle (RAB). (Image source: Wu WT et al., Ultrasonography 2022) [33]
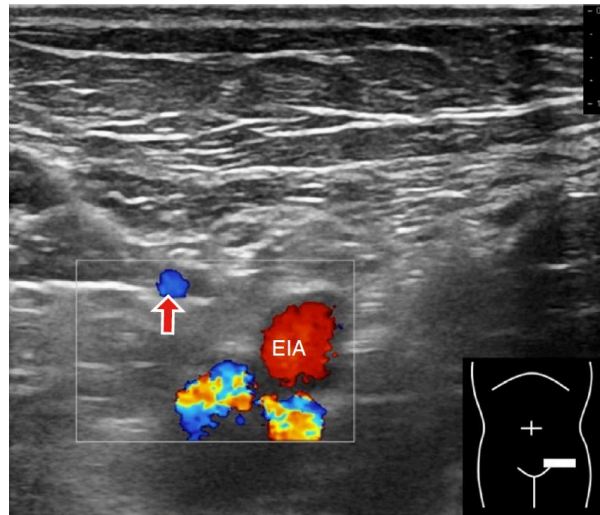
Figure 88: Visualisation of the inferior epigastric artery (red arrow). (Image source: Wu WT et al., Ultrasonography 2022) [33]
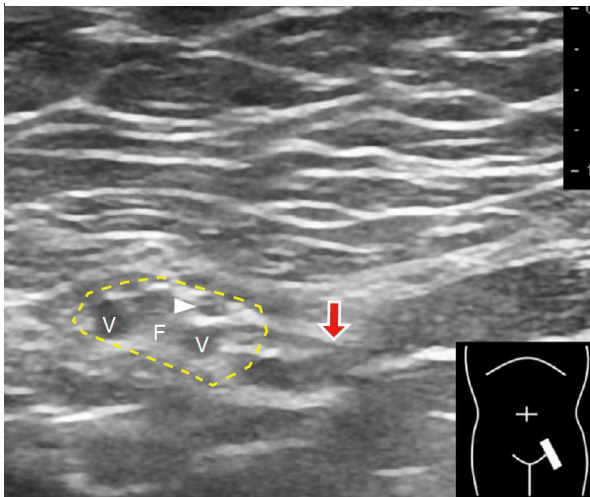
Figure 89: Cross section of the inguinal canal (yellow dashes). (Image source: Wu WT et al., Ultrasonography 2022) [33]
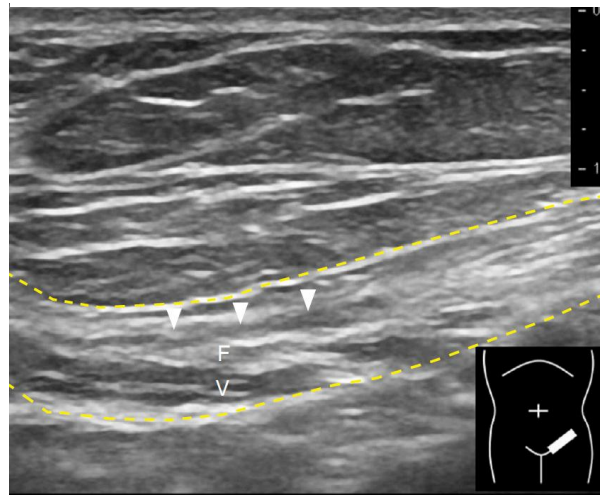
Figure 90: Longitudinal view of the inguinal canal. (Image source: Wu WT et al., Ultrasonography 2022) [33]

5.4.6.1. Case study of an indirect inguinal hernia

Figure 91: Longitudinal view of the hernial sac. White arrows: spermatic cord. Asterisk: Hernia consisting of peritoneal fatty tissue and intestine. (Image source: Wu WT et al., Ultrasonography 2022) [33]

Figure 92: Cross section of the hernial sac. Red arrow: Vasa testicularia. (Image source: Wu WT et al., Ultrasonography 2022) [33]

Male patient. Fig. 91 shows a longitudinal section of the hernia, consisting of peritoneal fatty tissue and intestine (asterisk). Fig. 92 shows a transverse section of the hernia.[33]

5.4.6.2. Case study of the Valsalva manoeuvre for indirect inguinal hernia
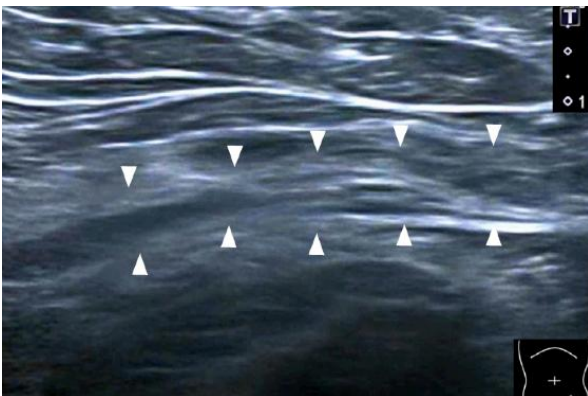
Figure 93: Longitudinal view of the inguinal canal (arrowheads) at rest. (Image source: Wu WT et al., Ultrasonography 2022) [33]
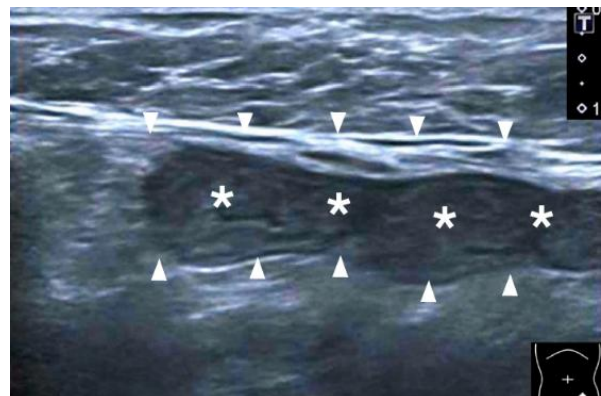
Figure 94: Longitudinal view of the same inguinal canal during Valsalva maneuver. A hernia is visible with peritoneal fatty tissue and bowel (asterisk) in the inguinal canal. (Image source: Wu WT et al., Ultrasonography 2022) [33]

The sex of this patient is unknown. A Valsalva compression test revealed a hernia sac in the inguinal canal running along it. This suggests an indirect inguinal hernia.[33]

5.4.6.3. Case study of a direct inguinal hernia
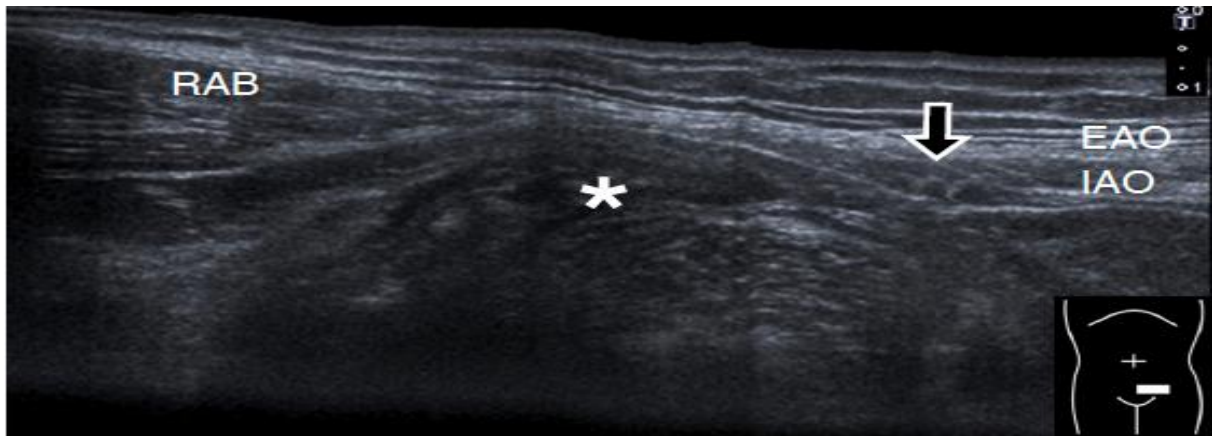
Figure 95: Transverse view over Hesselbach's triangle at rest. RAB: rectus abdominis muscle. Asterisk: hernia contents (bowel). Black arrow: Inferior epigastric artery. EAO: M.obliquus externus abdominis. IAO: M.obliquus internus abdominis. (Image source: Wu WT et al., Ultrasonography 2022) [33]
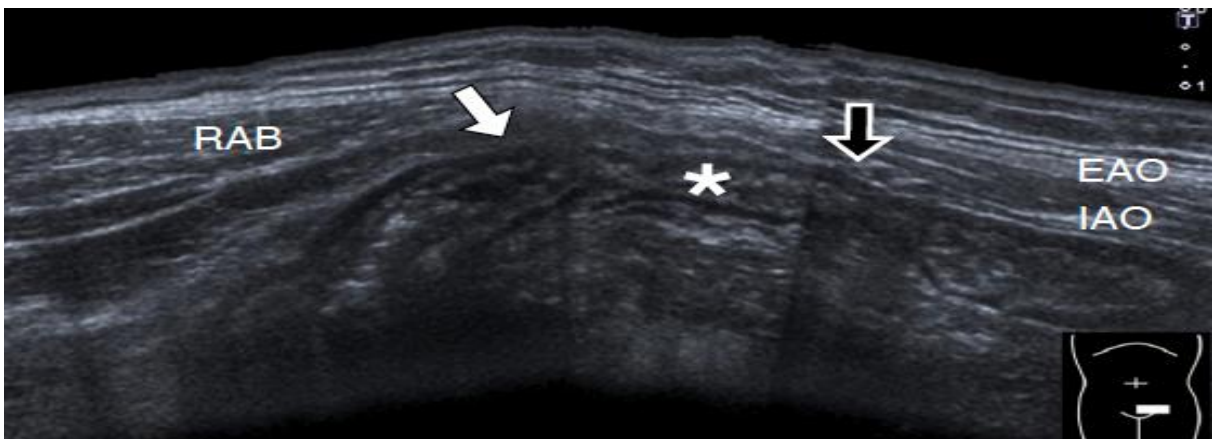
Figure 96: Transverse section at the same position during the Valsalva press test. An intestinal loop (asterisk) emerges through the hernial orifice (white arrow). (Image source: Wu WT et al., Ultrasonography 2022) [33]

Shown here is a case of a direct inguinal hernia. The contents of the hernia are pushed forward to the right edge of the image under Valsalva pressure. The reference to the inferior epigastric artery is helpful for orientation (Fig. 96, black arrow) . The sex of this patient is unknown.[33]

5.4.7. Patient case 10: Avulsion of the M. adductor longus

A 60-year-old man presented after a fall to the ground that led to a severe abduction of his right hip. The accident had happened two weeks before his visit to the doctor. He complained of slight pain in his right groin. An X-ray showed no evidence of an acute osseous lesion.[34]

The subsequent ultrasound examination revealed a fluid-filled defect replacing the insertion site of the adductor longus tendon. The tendon shows a retraction of 15 mm (Fig. 98). The myotendinous junction of the adductor longus is normal. In the adjacent pectineus muscle, there are some tiny fluid clefts with small areas showing a normal muscle echo pattern. The M. adductor brevis, adductor magnus and gracilis show a normal echo pattern. The contralateral adductor muscles were examined in comparison and were normal.[34]
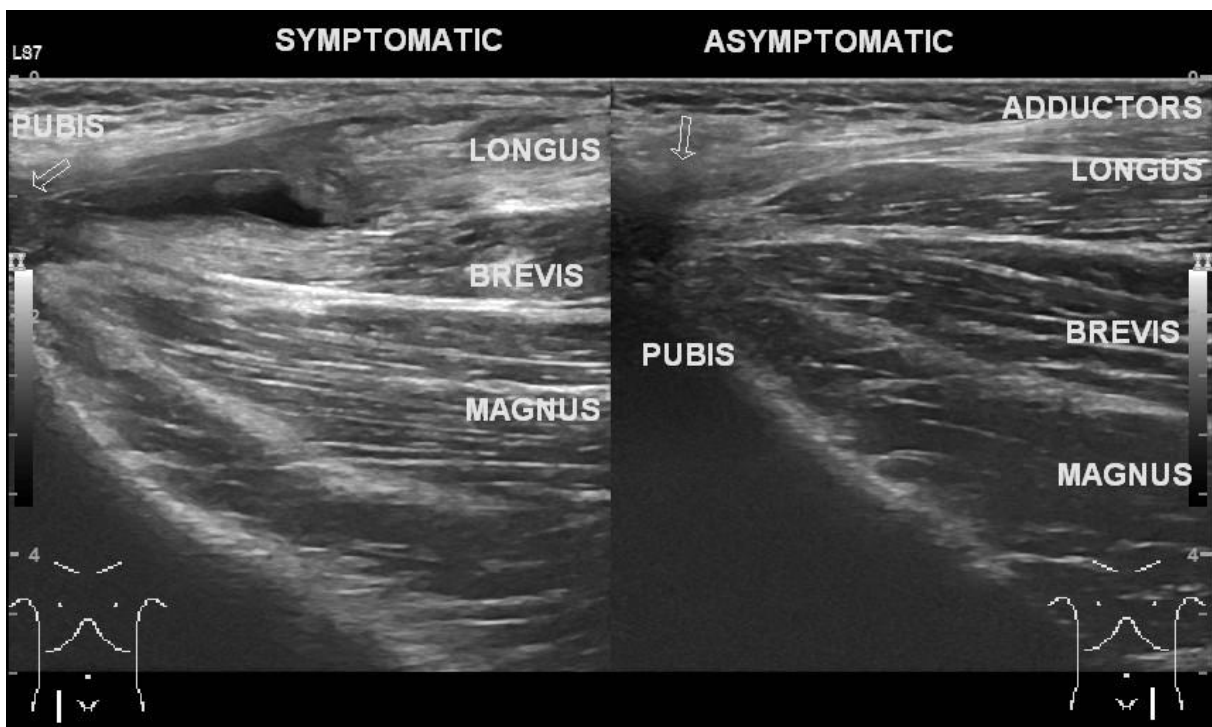
Figure 97: Longitudinal sections of the adductor regions in side-by-side comparison. (Image source: Patel M., 2021, radiopaedia.org) [34]

This case shows a complete rupture of the adductor longus tendon at its origin. In contrast to this case, adductor injuries are usually sports related.[34]
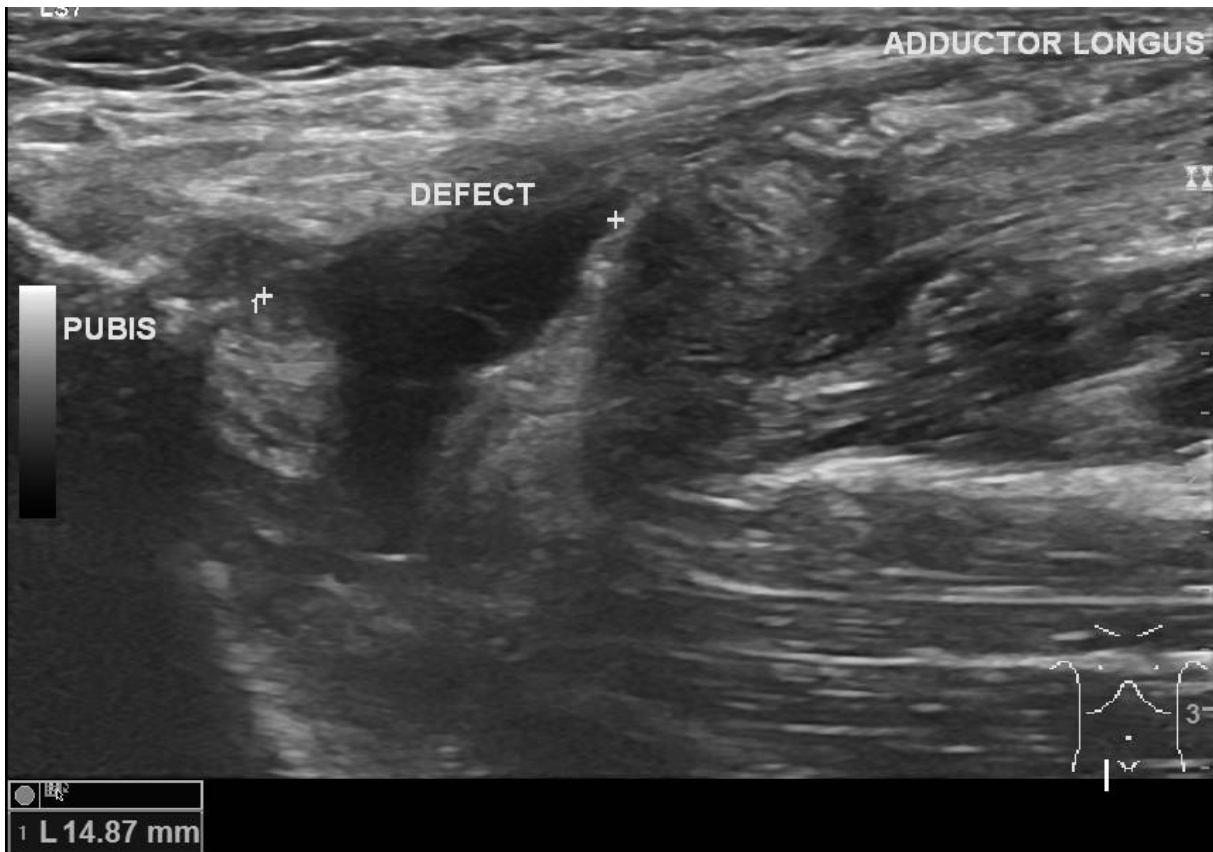
Figure 98: Longitudinal section of the symptomatic adductor muscles with an anechoic defect in the area of the adductor longus muscle. (Image source: Patel M., 2021, radiopaedia.org) [34]
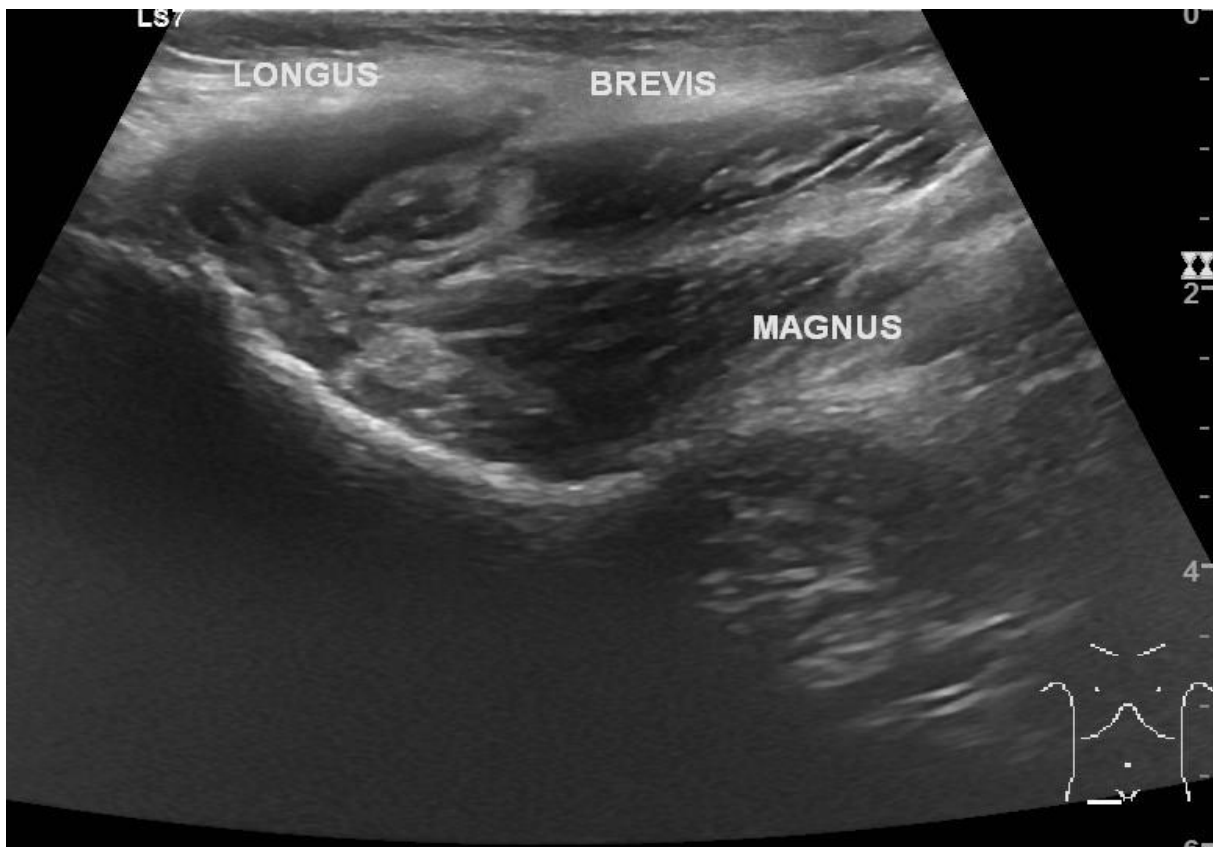
Figure 99: Cross-section of the symptomatic side with an anechoic defect in the area of the adductor longus. Graphic cropped. (Image source: Patel M., 2021, radiopaedia.org)[34]

5.4.8. Patient case 11: Septic arthritis of the hip

A seven-year-old boy presented with pain in his left hip. The pain had occurred two days ago during a martial arts lesson and had not changed since then. The physical examination revealed severe pain in the left hip. The patient was unable to walk. Laboratory tests revealed an elevated level of C-reactive protein. A bilateral hip ultrasound was performed.[35]
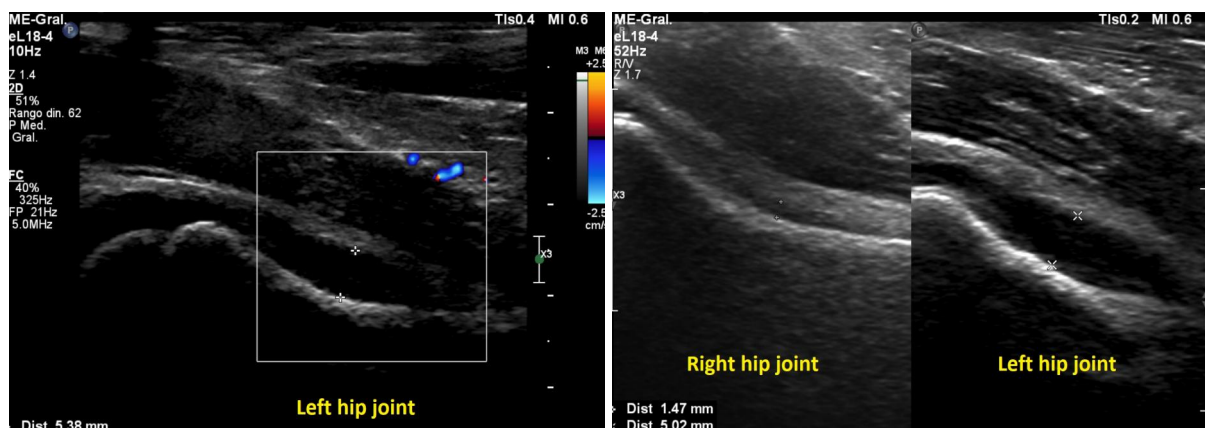
Figure 100: Longitudinal view in parallel axis tot he femoral neck of the affected side. An effusion is visible. (Image source: Jones J. et al., 2021, radiopaedia.org) [35]

Figure 101: Lateral comparison in the same section. The symptomatic side is shown on the right. (Image source: Jones J., et al., 2021, radiopaedia.org) [35]

Sonography revealed an effusion in the anterior recess of the left hip joint up to 5.4 mm. There was no hypervascularity of the neighbouring tissue. Intact femoral cortex. Normal right hip joint.[35]

A child with severe hip pain, elevated CRP and hip joint effusion is highly suspicious of septic arthritis. During surgery, pus was found in the left hip joint. Staphylococcus aureus was isolated from blood and hip joint effusion cultures. The absence of hypervascularity on power Doppler examination does not rule out septic arthritis.[35]

5.4.9. Patient case 12: Tear of the acetabular labrum

A child with severe hip pain, elevated CRP and hip joint effusion is highly suspicious of septic arthritis. During surgery, pus was found in the left hip joint. Staphylococcus aureus was isolated from blood and hip joint effusion cultures. The absence of hypervascularity on power Doppler examination does not rule out septic arthritis.[36]
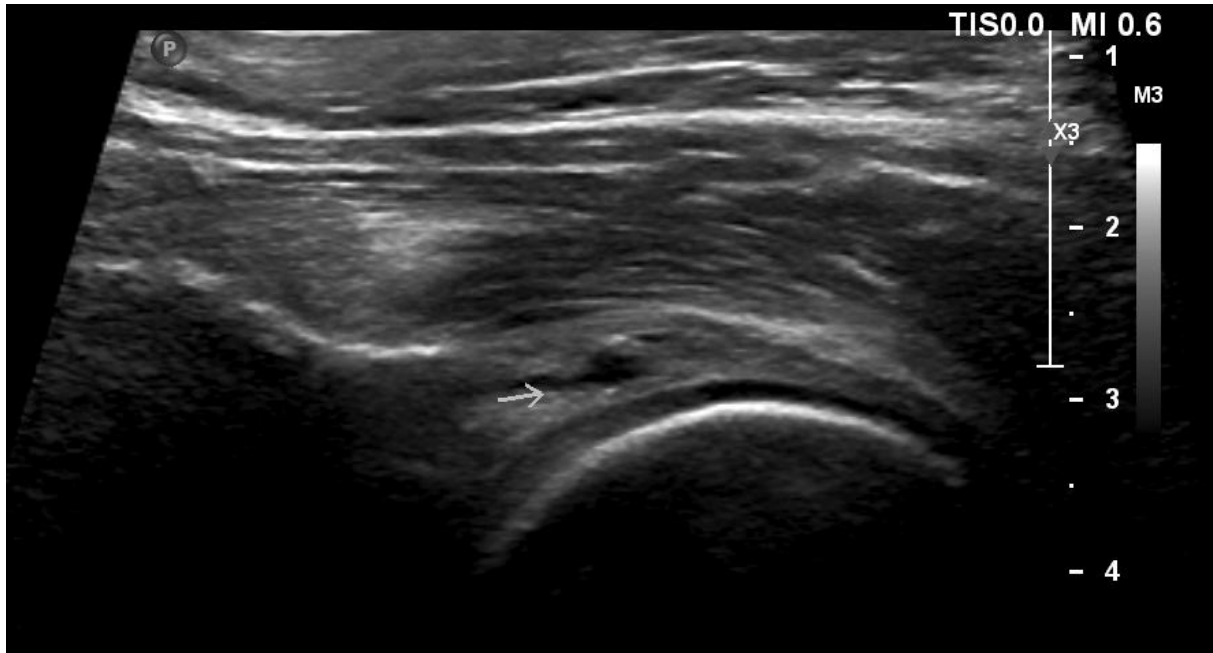
Figure 102: Sagittal view of the right hip joint. Arrow: Tear in the acetabular labrum. (Image source: Alkhateeb K., 2019, radiopaedia.org)[36]

Labral tears are a common finding in hip arthroscopy for hip pain (55%).[37]

A tear of the acetabular labrum can be asymptomatic but can also cause groin pain. Over time, labral tears can cause permanent hip damage.[36]

The current gold standard of treatment is hip arthroscopy, with labral tears being the main indication. Conservative therapies (NSAIDs, physiotherapy and intra-articular injections) are also available.[38]

5.5. Knee

5.5.1. Quadriceps tendon
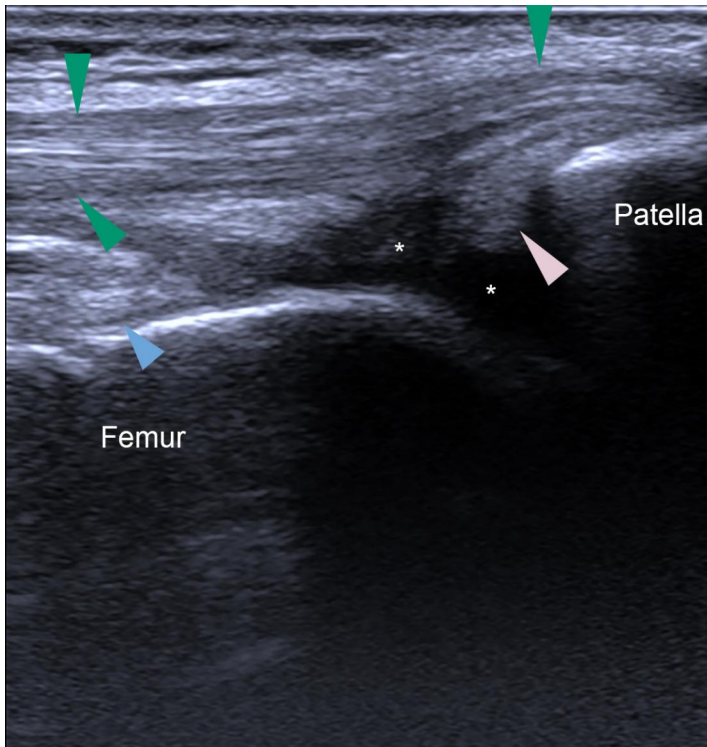
Figure 103: Sagittal view. Green arrows: Quadriceps tendon. Blue arrows: prefemoral fat pad. Pink arrows: suprapatellar fat pad. Asterisk: suprapatellar synovial recess.

Figure 104: Probe positioning.

To examine the quadriceps tendon, the patient is positioned in a lying or sitting position with approx. 30° flexion in the knee joint. A cushion can be placed under the knee joint for this purpose. The probe is placed sagittally directly proximal to the patella. The hyperechogenic line of the patella should be visible at the distal edge of the image. Directly anterior to the femur is the prefemoral fat pad (Fig. 103, blue arrow), recognisable as a larger hyperechogenic mass. A second fat pad is located proximal to the patella (suprapatellar fat pad, Fig. 103, pink arrow). In between lies the suprapatellar synovial recess, which is slender and slightly S-shaped in healthy patients. Larger pathological effusions can be detected here even at rest. Isometric contraction of the quadriceps by the patient or compression of the parapatellar recess with the examiner's free hand can also detect smaller joint effusions, as the fluid escapes cranially. A distinction can be made between synovial thickening and a questionable effusion by applying pressure to the probe. If the finding is displaceable, it is an effusion, otherwise it is synovial thickening. The probe should also be moved medially and laterally so as not to miss smaller effusions.[39]

5.5.2. **Trochlea femoralis**
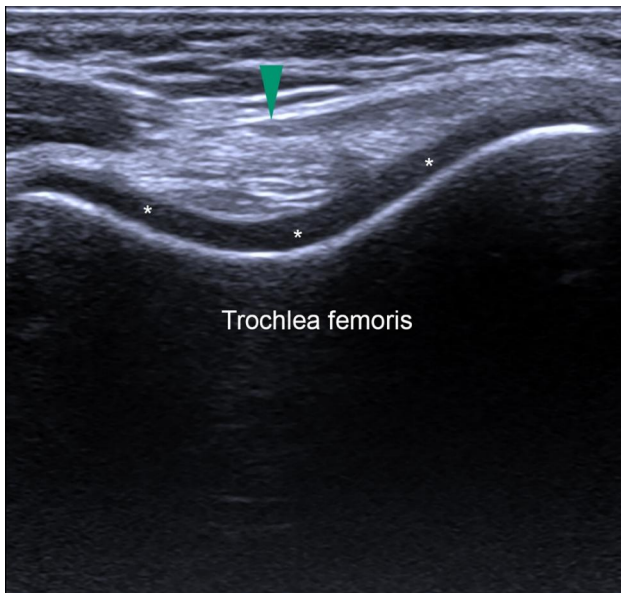
Figure 105: Transverse view. Asterisk: Articular cartilage of the trochlea. Green arrow: quadriceps tendon.
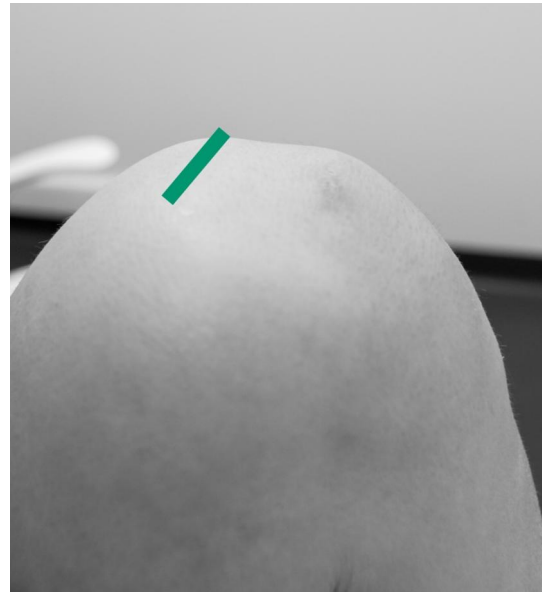
Figure 106: Probe positioning.

To examine the trochlea, the knee is fully flexed. The probe is placed transversely above the patella. The cartilage (Fig. 105, asterisk) and the quadriceps tendon (Fig. 105, green arrow) can be assessed here.[39]

5.5.3. Patellar tendon
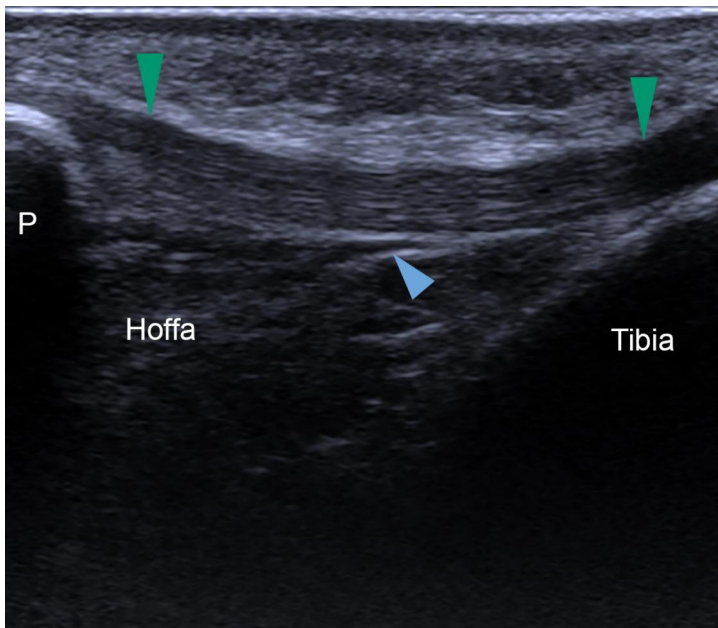
Figure 107: Sagittal view. P: Patella. Green arrows: patellar tendon. Blue arrow: bursa infrapatellaris profunda.

Figure 108: Probe positioning.

To examine the patellar tendon, the patient is again positioned with the knee in 30° flexion. The probe is placed on the apex patellaris (Fig. 107, left, P) and then rotated around this fixed point until the entire length of the patellar tendon is visible. The tendon can be assessed in this way, as can the Hoffa's fat body, which lies posterior to the tendon. Caution: The origin of the patellar tendon forms a V-shape around the apex. This region should also be examined so as not to miss any tendinopathy.[39]

A slight enlargement of the infrapatellar bursa profunda (Fig. 107, blue arrow) is physiological and can be visualised as a small triangular hypoechogenic area. The superficial infrapatellar bursa cannot normally be visualised.[39]

5.5.4. Medial collateral ligament
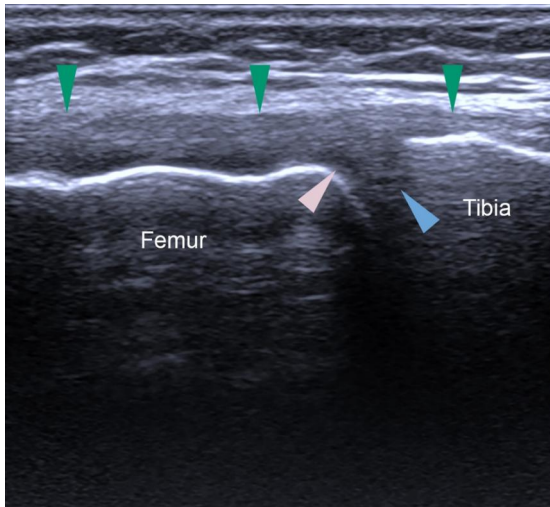
Figure 109: Longitudinal view of the medial collateral ligament (green arrows). Blue arrow: medial meniscus. Pink arrow: Meniscofemoral ligament.
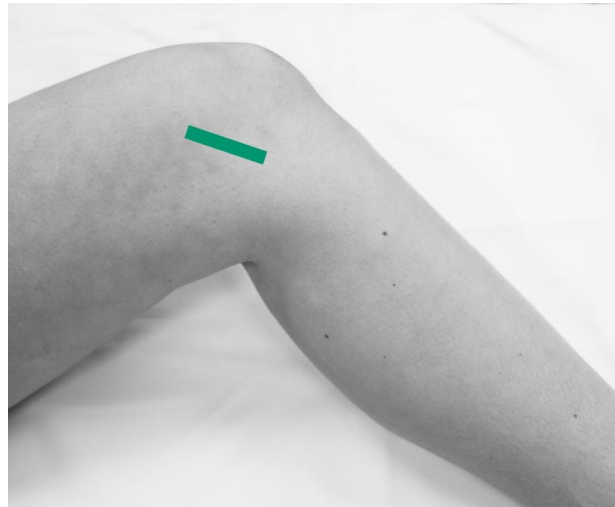
Figure 110: Probe positioning.

To examine the medial aspects of the knee, the leg is externally rotated while maintaining a flexion of 30°. The probe is positioned in the expected longitudinal axis of the medial collateral ligament. It is often necessary to move the probe distally and proximally for a full-length examination as the tendon is usually longer than the ultrasound probe. Valgus stress can be helpful in assessing a suspected ligament lesion. The outer part of the medial meniscus can also be viewed here.[39]

5.5.5. Lateral collateral ligament
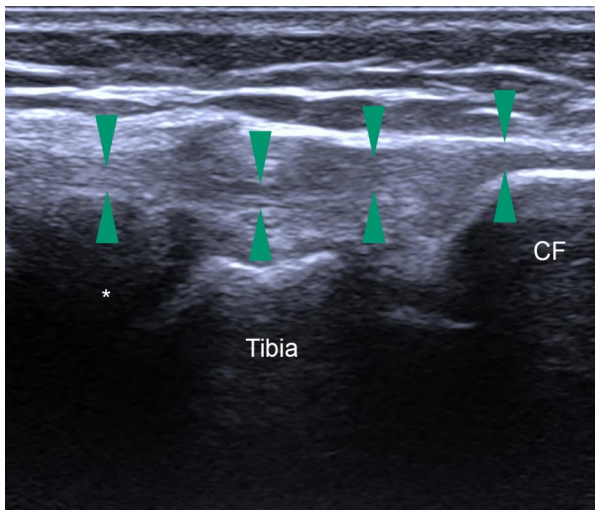
Figure 111: Longitudinal view of the lateral collateral ligament (green arrows). Asterisk: lateral meniscus. CF: Caput fibulae.
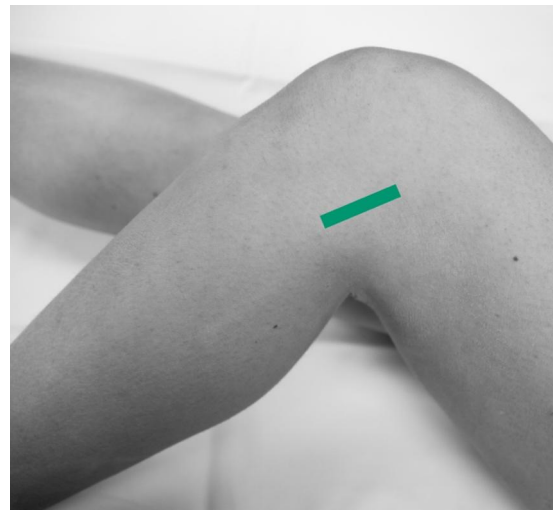
Figure 112: Probe positioning.

To examine the lateral collateral ligament, the leg is internally rotated while maintaining 30° flexion. The probe is then placed in the longitudinal axis of the expected ligament extension. For correct positioning, the fibular head can be used as a distal reference point (Fig. 111, right, CF), then the probe is rotated around this fixed point until the ligament is visible in its greatest length in the image.[39]

The outer portion of the meniscus (Fig. 111, asterisk) can also be seen here. If a meniscus cyst is suspected, the examination can be repeated with the knee in forced flexion, as the fluid is pressed laterally.[39]

In the area of the tibiofibular joint, joint effusions and paraarticular ganglia can be searched for.[39]

5.5.6. Intercondylar fossa
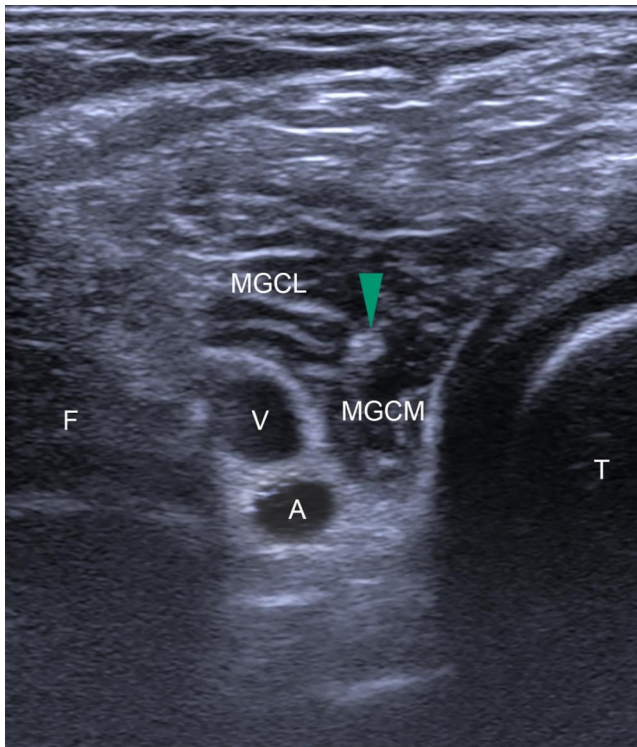
Figure 113: Transverse view. F: Femur. MGCL: M.gastrocnemius, caput mediale. V: V.poplitea. A: A.poplitea. MGCM: M.gastrocnemius, caput laterale. T: Tibia. Green arrow: N.tibialis.

Figure 114: Probe positioning.

To examine the popliteal nerve-vessel bundle, the patient is asked to lie in the prone position. The probe is placed in the transverse direction at the level of the knee bend. By moving it proximally and distally, the popliteal artery can be visualised in depth, the popliteal vein in the middle and the posterior tibial nerve (Fig. 113, green arrow). If the popliteal vein cannot be seen, the knee can be slightly flexed, which fills the vein and makes it easier to visualise.[39]

5.5.7. Patient case 13: Quadriceps tendon rupture

A 50-year-old man presented 4 months after trauma to the anterior distal third of the left thigh. He had a non-MRI-compatible prosthetic heart valve.[40]

There was a complete rupture of the quadriceps tendon. Retraction from the patella (~5 cm). The defect showed a small amount of anechoic fluid and a prolapse of the subcutaneous fatty tissue.[40]
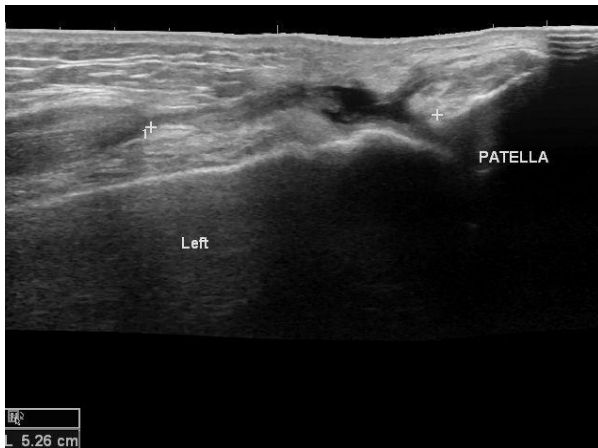
Figure 115: Longitudinal section of the quadriceps tendon on the affected side. The tendon is clearly retracted from the patella. Panoramic image. (Image source: Patel M., 2011, radiopaedia.org) [40]

5.5.8. Patient case 14: Tendosynovial giant cell tumour

A 20-year-old female presented with anterior swelling of the left knee for the past few months. She reported mild localised pain.[41]

The ultrasound examination showed a well-defined lesion in the area of the swelling, measuring approx. 19 x 16 x 13 mm. The lesion was located in the subcutaneous plane. It was separate from the joint and located medial to the patellar tendon. The lesion was hypoechogenic, slightly heterogeneous and showed no calcification or cystic changes. There was posterior acoustic enhancement. It showed slight compressibility. There were a few flow signals in the peripheral part of the lesion. The quadriceps and patellar tendons were normal. There was no effusion in the suprapatellar region.[41]

The lesion was surgically excised. Histopathology revealed a tendosynovial giant cell tumour.[41]
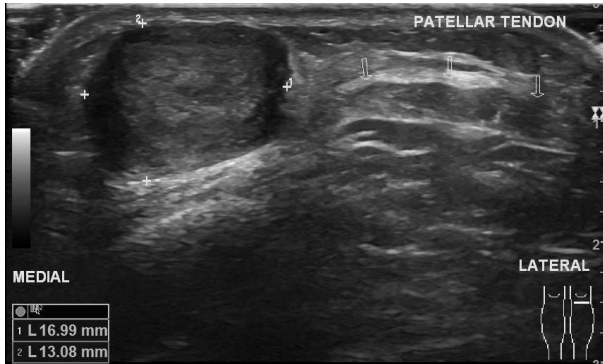
Figure 116: Visualisation of the lesion in transverse plane. (Image source: Bickle I. et al., 2019, radiopaedia.org) [41]

Figure 117: Visualisation of the lesion in sagittal view just medially of the patellar tendon. (Image source: Bickle I. et al., 2019, radiopaedia.org) [41]

5.5.9. Patient case 15: Infrapatellar bursitis

A 25-year-old woman presented with pain in her left anterior knee that had been present for two days. There had been no trauma. No X-ray was performed as the patient was 8 weeks pregnant. The ultrasound examination showed an anechoic fluid accumulation at the site of pain reported by the patient. The fluid was located at the site of the deep infrapatellar bursa. The patellar tendon, Hoffa's fat pad and quadriceps tendon were normal. There was no effusion in the suprapatellar recess of the knee joint.[42]

Ultrasound revealed an infrapatellar bursitis, which explained the symptoms satisfactorily.[42]
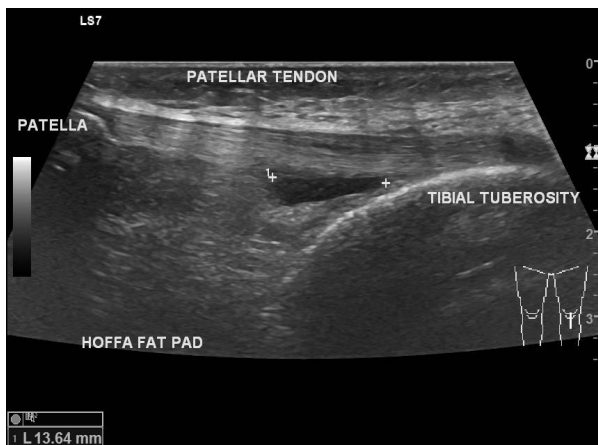
Figure 118: Sagittal view. Anechoic fluid collection posterior to the patellar tendon. (Image source: Patel M., 2021, radiopaedia.org) [42]
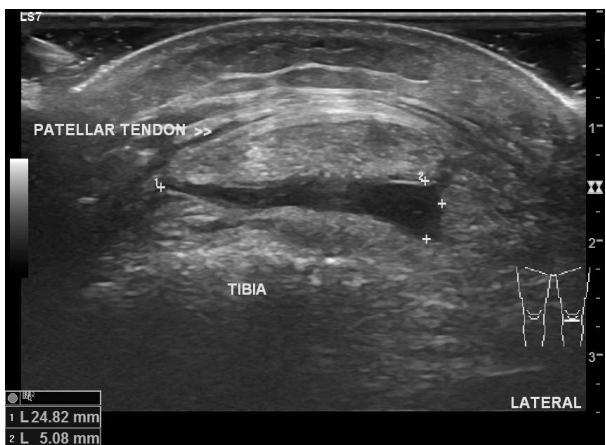
Figure 119: Transverse view of the affected side. (Image source: Patel M., 2021, radiopaedia.org) [42]

5.6. Ankle

To examine the ankle joints, the patient is asked to sit on the examination table and flex the knee 45° so that the sole of the foot can be placed on the table.[43]

5.6.1. Anterior ankle joint surface
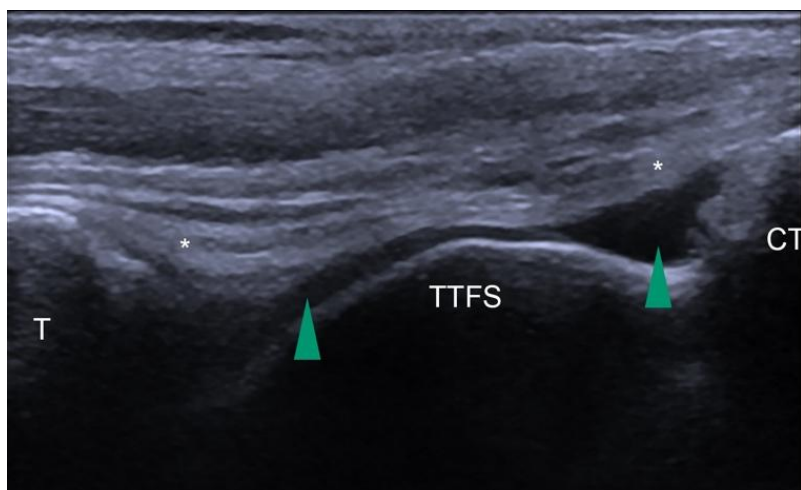
Figure 120: Sagittal view. T: Tibia. Asterisk: Anterior fat pad. Green arrows: Anterior recess of the tibiotalar joint. TTFS: Trochlea talaris, facies superior. CT: Caput tali.
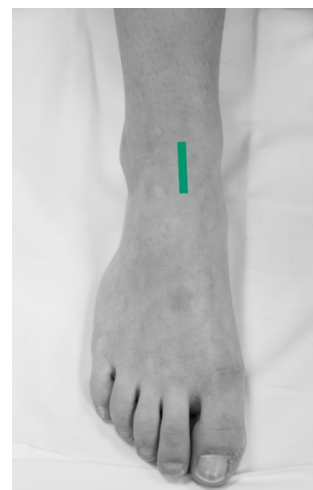
Figure 121: Probe positioning.

To examine the anterior ankle joint, the probe is positioned in the sagittal plane in the direction of the second beam. By moving the probe medially and laterally, fluid can be searched for in the anterior recess of the tibiotalar joint..[43]

5.6.2. Lig. talofibulare anterius
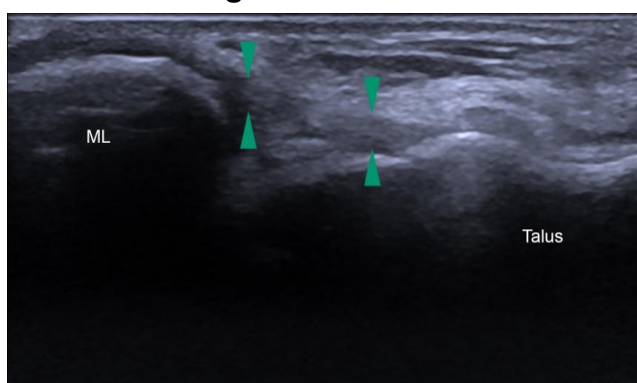
Figure 122: Longitudinal view of the Lig. talofibulare anterius (green arrows). ML: Malleolus lateralis.
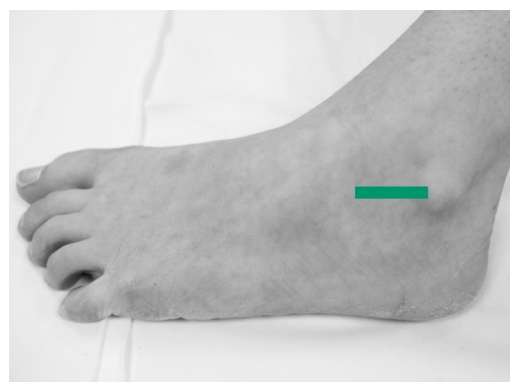
Figure 123: Probe positioning.

To examine the anterior talofibular ligament, the foot is slightly inverted (internally rotated) to stretch the lateral ligaments. The probe is placed parallel to the examination table, with the proximal end resting on the lateral malleolus.[43]

5.6.3. Anterior tibiofibular ligament
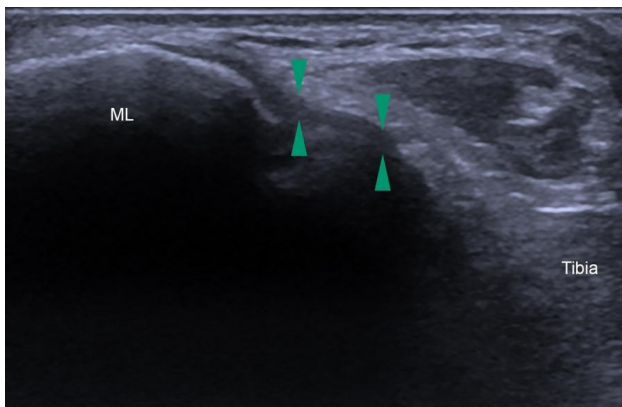
Figure 124: Longitudinal view of the anterior tibiofibular ligament (green arrows). ML: Malleolus lateralis.
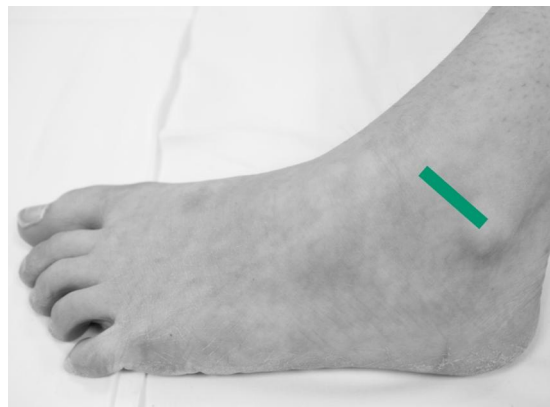
Figure 125: Probe positioning.

To examine the anterior tibiofibular ligament, the probe can be rotated cranially (clockwise) from the position described above while maintaining the anchor point on the lateral malleolus until the entire length of the anterior tibiofibular ligament can be viewed.[43]

5.6.4. Peroneal tendons
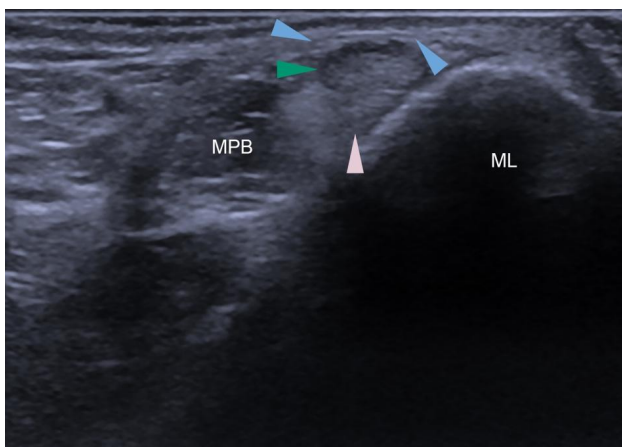
Figure 126: Cross section of the peroneal tendons.. MPB: M.peroneus brevis. Green arrow: tendon of the M.peroneus longus. Pink arrow: tendon of the M.peroneus brevis. Blue arrow: Upper extensor retinaculum. ML: Malleolus lateralis.
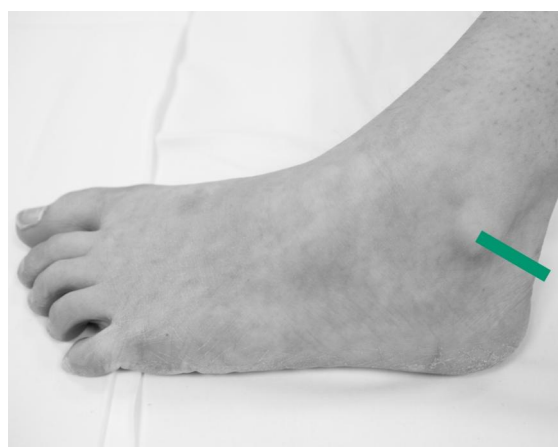
Figure 127: Probe positioning.

To examine the peroneal tendons, the probe is placed directly posterior to the lateral malleolus so that the malleolus is still cut at the anterior edge of the image. The tendons are examined by moving the probe parallel to their course.[43]

5.6.5. Deltoid ligament
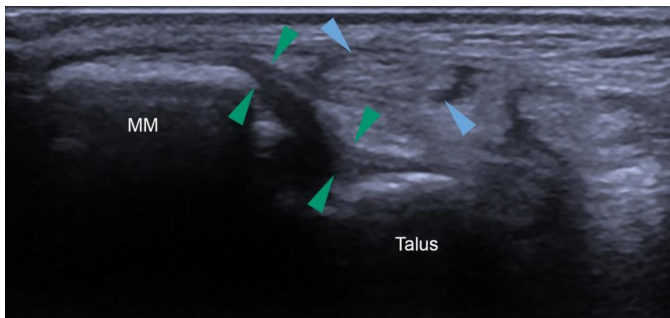
Figure 128: MM: Malleolus medialis. Green arrows: Lig.tibiotalare. Blue arrows: Tendon of the M.tibiale posterius
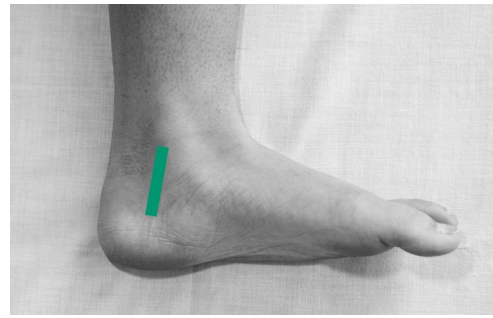
Figure 129: Probe positioning.

To examine the posterior part of the deltoid ligament, the foot is tilted laterally by rotating outwards in the hip while maintaining flexion in the knee until the lateral edge of the foot comes to rest on the examination table. In addition, the foot must be dorsiflexed as far as possible. The probe is placed slightly distal to the medial malleolus in a slightly rotated (clockwise) coronal plane so that the proximal end lies over the malleolus and the distal end of the probe is moved anteriorly or posteriorly (counterclockwise or clockwise rotation) until the ligament can be visualised in its longitudinal axis.[43]

5.6.6. Achilles tendon
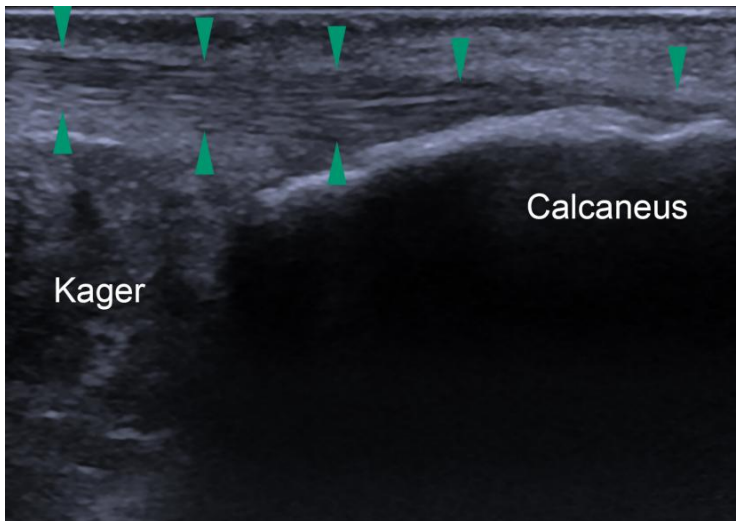
Figure 130: Longitudinal view of the achilles tendon (green arrows). Kager: Kager fat body.

Figure 131: Probe positioning.

To visualise the Achilles tendon, the patient is asked to lie in a prone position. The foot should protrude over the table so that the OSG can be freely flexed/extended. The probe is then placed in the sagittal plane from the dorsal side so that the distal end of the probe comes to rest over the calcaneus. In this view, the insertion of the Achilles tendon and the anterior-proximal Kager fat body can be visualised. The length of the Achilles tendon is then traced up to the myotendinous junction and checked for signs of rupture.[43]

5.6.7. Plantar fascia
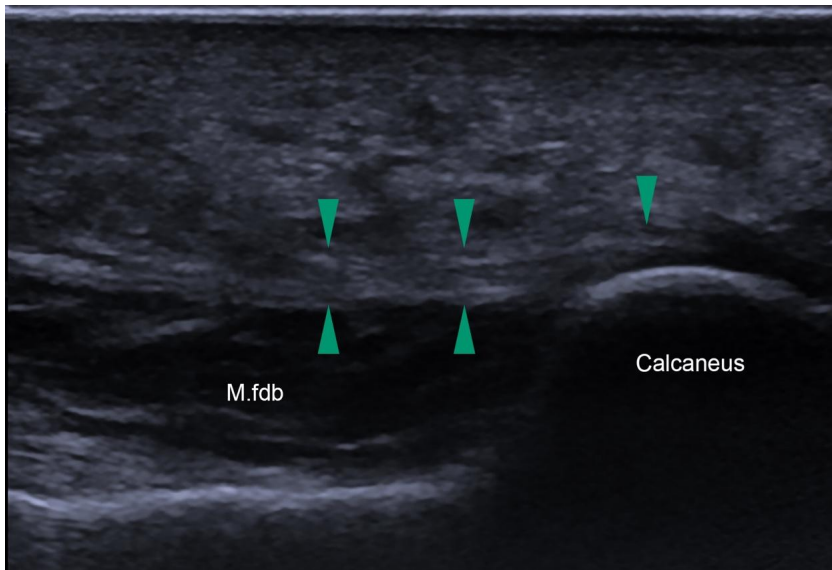
Figure 132: Longitudinal view of the plantar fascia (green arrows). M.fdb: M.flexor digitorum brevis.
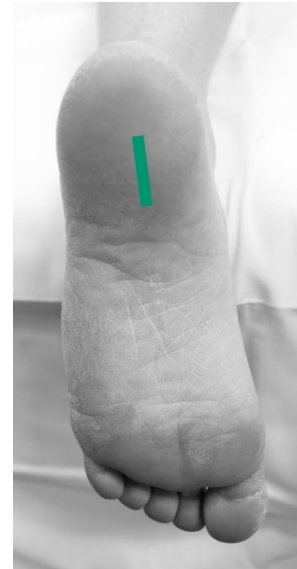
Figure 133: Probe positioning.

To examine the plantar fascia, the patient can be left in the same position. The probe is placed in the sagittal axis plantar above the heel just medial to the midline so that the calcaneus, recognisable as a convex line with a rich echo, appears on the right edge of the image (Fig. 132, right). [43]

5.6.8. Patient case 16: Rupture of the anterior talofibular ligament

A 20-year-old female presented a few hours after an inversion injury to her right foot. She complained of difficulty walking and lateral pain and swelling of the affected ankle. An X-ray did not reveal a fresh osseous lesion but showed a discrete widening of the lateral joint space.[44]

Sonography revealed a complete rupture of the anterior talofibular ligament near the fibular insertion. The rest of the ligament showed a normal echo pattern. The anterior recess of the ankle showed an effusion and lateral subcutaneous oedema.[44]
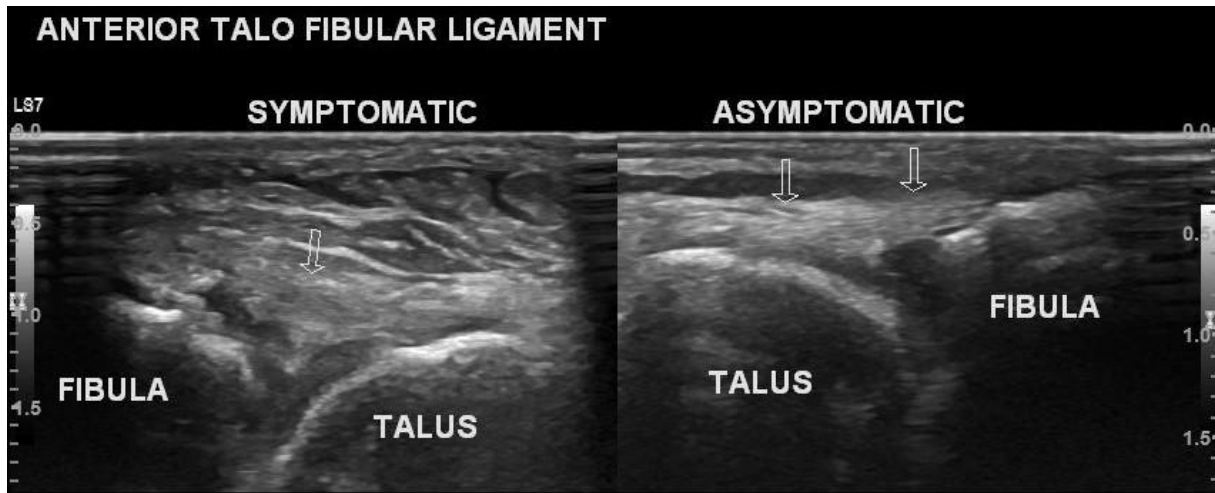
Figure 134: Anterior talofibular ligament, longitudinal section with comparison with the opposite side. (Image source: Patel M., 2019, radiopaedia.org) [44]

Figure 135: Sagittal view of the anterior ankle joint. The effusion can be seen posterior tot he arrows. (Image source: Patel M., 2019, radiopaedia.org) [44]

5.6.9. Patient case 17: Achilles tendon rupture

A 40-year-old male presented following trauma to his left Achilles tendon. The patient complained of pain in the area of the Achilles tendon.[45]

The ultrasound examination showed a complete (in thickness and width) tear of the Achilles tendon. The tear was located 60 mm proximal to the tendon insertion. There was a gap of 25 mm between the two edges of the torn tendon. The defect was filled with fluid, with the echo pattern indicating haemorrhage. The tendon proximal and distal to the tear showed a normal echo pattern. There was a tiny enthesophyte at the insertion. The asymptomatic tendon was intact and showed a normal echo pattern.[45]

Figure 136: Sagittal section of the affected (left) side. Panoramic image. (Image source: Patel M., 2020, radiopaedia.org) [45]

Figure 137: Transverse section of the affected side. (Image source: Patel M., 2020, radiopaedia.org) [45]

5.6.10. Patient case 18: Longitudinal tear of the peroneus brevis muscle

A 35-year-old male presented two months after injuring his left ankle. He complained of pain in the area of the lateral ankle and an occasional cracking sound. Ultrasound examination revealed a longitudinal transection of the peroneus brevis tendon in the area of the retromalleolar groove and just distal to the lateral malleolus. The length of the tear was approximately 35 mm (measurement not shown in source). No tenosynovitis was visible. The proximal muscle belly and the distal tendon insertion were normal. The peroneus longus tendon and muscle belly were normal. No injury to the peroneal retinaculum was visible. No subluxation/luxation of the brevis/longus tendon in relation to the retromalleolar groove. The calcaneofibular ligament was normal.[46]

Figure 138: Peroneal tendons of the affected side in cross-section. (Image source: Patel M., 2023, radiopaedia.org) [46]
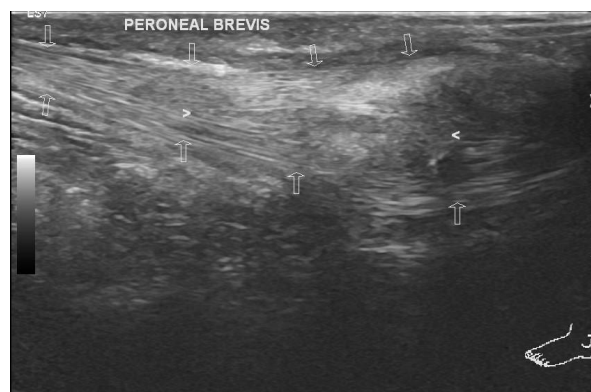
Figure 139: Tendon of the peroneus brevis muscle in longitudinal section at the level of the rupture. (Image source: Patel M., 2023, radiopaedia.org) [46]

This case shows a split tear (longitudinal tear) of the tendon of the peroneus brevis muscle. The presence of three structures in the retromalleolar groove could be an indication of an additional peroneal muscle; however, this is unlikely in the context of the symptoms.[46]

5.6.11. Patient case 19: Instability of the peroneal tendons

This case shows a retromalleolar intrareticular peroneal tendon subluxation in a young skier that was not recognisable on MRI and could be detected on a dynamic ultrasound examination.

a. Transverse section at the level of the lateral malleolus with the ankle joint in neutral position shows the tendons of the peroneus longus (L) and the peroneus brevis (B) in anatomical position. The arrow points to a slightly thickened superior retinaculum.

b. During active eversion of the ankle, the tendons abruptly change their position in the retromalleolar groove. Note the increasing laxity of the superior retinaculum (arrow).

c. When the ankle joint is in the neutral position the tendons change abruptly again into their anatomical position [47]
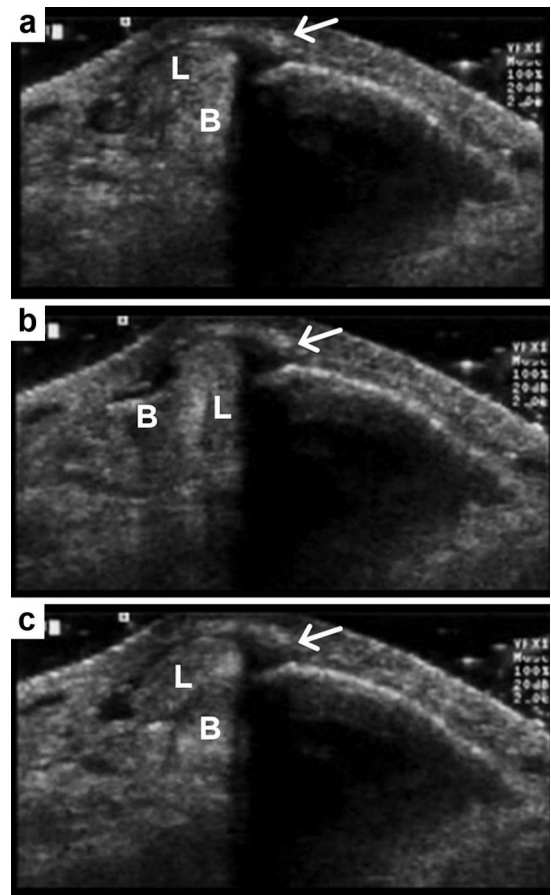
Figure 140: Transverse section in the area of the lateral malleolus. Dynamic examination.
(Image source: Bureau NJ et.al., Curr Radiol Rep., 2016) [47]

6. Discussion and Conclusion

This work shows the most important standard sections of relevant questions in musculoskeletal ultrasound of the wrist, elbow, shoulder, hip, knee and ankle. Exemplary images with descriptions of the sections and anatomical structures were created and the positioning of the patient explained. Several patient cases per region were also presented and explained in order to place the described procedures in a clinical context. The advantages and disadvantages of the imaging procedures were explained and compared.

MSK ultrasound is particularly strong in the visualisation of superficial structures, whereby this form of imaging is superior to other imaging procedures in some cases. In addition, the detection of inflammation, for example, is not only possible via indirect signs (e.g. free fluid or abscess) compared to computer tomography. In addition, the hyperperfusion caused by inflammation can be visualised directly at the affected site using Doppler examination.

Even in the case of functional restrictions such as shoulder impingement or tendon instability (see section 4.6.11: Patient case 19), which are difficult to visualise using other imaging techniques, the tissue can be viewed and moved in vivo using a dynamic examination. This can lead to a better understanding of the pathology and a more precise diagnosis. MSK sonography therefore proves to be a valuable addition to everyday clinical practice.

The focus of the work was the presentation of common standard ultrasound incisions in the MSK area. The intention to keep this guide clear and to cover the common pathologies is limited by the fact that not all sections could be covered. In a future work, further, less frequently used incisions could be shown in order to cover a broader spectrum of possible pathologies. For example, sections of the thorax (such as the thoracolumbar fascia or areas of the spine and lumbar region) could also be shown.

A further question is whether MSK ultrasound can save or replace an MRI or CT examination in certain cases. As discussed in the introduction, this would be an advantage from the patient's point of view and in economic terms. Further studies investigating this aspect would be valuable.

7. Conflict of interest

The authors declare that there were no conflicts of interest within the meaning of the recommendations of the International Committee of Medical Journal Editors when the article was written.

8. Disclaimer / Publisher's Note

The statements, opinions and data contained in all publications are solely those of the individual author(s) and contributor(s) and not of Swiss J. Radiol. Nucl. Med. and/or the editor(s). Swiss J. Radiol. Nucl. Med. and/or the editor(s) disclaim responsibility for any injury to people or property resulting from any ideas, methods, instructions or products referred to in the content.

9. License Policy

This work is licensed under a Creative Commons Attribution 4.0 International License. This license requires that reusers give credit to the creator. It allows reusers to distribute, remix, adapt, and build upon the material in any medium or format, even for commercial purposes.

10. Correspondence to

Dan Tschanz - https://orcid.org/0009-0008-0608-0933

Department of Diagnostic, Interventional and Pediatric Radiology (DIPR), Inselspital, Bern University Hospital, University of Bern, Switzerland

11. Bibliography

1. Sharpe RE, Nazarian LN, Parker L, Rao VM, Levin DC. Dramatically increased musculoskeletal ultrasound utilization from 2000 to 2009, especially by podiatrists in private offices. Journal of the American College of Radiology 2012;9(2):141–6.

2. Middleton WD, Payne WT, Teefey SA, Hildebolt CF, Rubin DA, Yamaguchi K. Sonography and MRI of the Shoulder: Comparison of Patient Satisfaction. American Journal of Roentgenology [Internet] 2004 [cited 2023 Oct 27];183(5):1449–52. Available from: https://pubmed.ncbi.nlm.nih.gov/15505319/

3. Hofer Matthias. Sono Grundkurs. 11th ed. Stuttgart: Georg Thieme Verlag; 2023.

4. Narouze Samer N. Atlas of Ultrasound-Guided Procedures in Interventional Pain Management [Internet]. New York, NY: Springer New York; 2011. Available from: http://link.springer.com/10.1007/978-1-4419-1681-5

5. Nazarian LN. The Top 10 Reasons Musculoskeletal Sonography Is an Important Complementary or Alternative Technique to MRI. American Journal of Roentgenology [Internet] 2008 [cited 2023 Oct 27];190(6):1621–6. Available from: https://www.ajronline.org/doi/10.2214/AJR.07.3385#sec-3

6. Bangard C, Paszek J, Berg F, et al. MR imaging of claustrophobic patients in an open 1.0T scanner: Motion artifacts and patient acceptability compared with closed bore magnets. Eur J Radiol [Internet] 2007 [cited 2023 Oct 27];64(1):152–7. Available from: https://pubmed.ncbi.nlm.nih.gov/17374468/

7. Neumann T, Ermert H. Schlieren visualization of ultrasonic wave fields with high spatial resolution. Ultrasonics 2006;44(SUPPL.).

8. Link TM, Majumdar S, Peterfy C, et al. HIGH RESOLUTION MRI OF SMALL JOINTS: IMPACT OF SPATIAL RESOLUTION ON DIAGNOSTIC PERFORMANCE AND SNR. 1998.

9. Beggs I, Stefano Bianchi U, Angel Bueno S, et al. European Society of MusculoSkeletal Radiology Musculoskeletal Ultrasound Technical Guidelines I. Shoulder. 2010.

10. Khoury V, Cardinal É, Bureau NJ. Musculoskeletal Sonography: A Dynamic Tool for Usual and Unusual Disorders. American Journal of Roentgenology [Internet] 2007 [cited 2023 Oct 27];188(1):W63–73. Available from: https://www.ajronline.org/doi/10.2214/AJR.06.0579

11. Beggs I, Stefano Bianchi U, Angel Bueno S, et al. European Society of MusculoSkeletal Radiology Musculoskeletal Ultrasound Technical Guidelines II. Elbow. 2010.

12. Neustadter J, Raikin SM, Nazarian LN. Dynamic Sonographic Evaluation of Peroneal Tendon Subluxation. American Journal of Roentgenology [Internet] 2004 [cited 2023 Oct 27];183(4):985–8. Available from: https://pubmed.ncbi.nlm.nih.gov/15385290/

13. O'Neill J. Musculoskeletal ultrasound: Anatomy and technique. Springer New York; 2008.

14. Elshimy A, Osman AM, Awad MES, Abdel Aziz MM. Diagnostic accuracy of point-of-care knee ultrasound for evaluation of meniscus and collateral ligaments pathology in comparison with MRI. Acta radiol 2023;64(7):2283–92.

15. Gatz M, Bode D, Betsch M, et al. Multimodal Ultrasound Versus MRI for the Diagnosis and Monitoring of Achilles Tendinopathy: A Prospective Longitudinal Study. Orthop J Sports Med 2021;9(4):232596712110068.

16. Nischal N, Gupta S, Lal K, Singh JP. Performance Evaluation of High-Resolution Ultrasound versus Magnetic Resonance Imaging in Diagnosing Peripheral Nerve Pathologies. Indian Journal of Radiology and Imaging 2021;31(01):043–8.

17. Bachta A, Rowicki K, Kisiel B, et al. Ultrasonography versus magnetic resonance imaging in detecting and grading common extensor tendon tear in chronic lateral epicondylitis. PLoS One 2017;12(7):e0181828.

18. Murphy A, Morgan M. Musculoskeletal ultrasound [Internet]. Radiopaedia.org. 2014 [cited 2023 Oct 27];Available from: https://radiopaedia.org/articles/31803

19. Elliot Duff et al. Medical Ultrasound [Internet]. Wikipedia.org. 2002 [cited 2023 Dec 8];Available from: https://en.wikipedia.org/w/index.php?title=Medical_ultrasound&oldid=1182553254

20. Page P, Manske RC, Voight M, Wolfe C. MSK Ultrasound - An IJSPT Perspective. Int J Sports Phys Ther 2023;18(1).

21. Stanislavsky A, Patel M. Biceps long head tendon tear [Internet]. Radiopaedia.org. 2019 [cited 2023 Nov 8];Available from: https://radiopaedia.org/cases/65346

22. Patel M. Lipoma - subdeltoid [Internet]. Radiopaedia.org. 2023 [cited 2023 Nov 8];Available from: https://radiopaedia.org/cases/163404

23.   Jin T, Patel M. Supraspinatous tendon tear [Internet]. Radiopaedia.org. 2010 [cited 2023 Nov 8];Available from: https://radiopaedia.org/cases/12576

24.   Botz B. High grade rupture of the distal triceps tendon [Internet]. Radiopaedia.org. 2022 [cited 2023 Nov 6];Available from: https://radiopaedia.org/cases/98612

25.   Patel M. Anconeus epitrochlearis [Internet]. Radiopaedia.org. 2020 [cited 2023 Nov 6];Available from: https://radiopaedia.org/cases/84506

26.   Patel M. Medial elbow snapping [Internet]. Radiopaedia.org. 2023 [cited 2023 Nov 6];Available from: https://radiopaedia.org/cases/166258

27.   Beggs I, Stefano Bianchi U, Angel Bueno S, et al. European Society of MusculoSkeletal Radiology Musculoskeletal Ultrasound Technical Guidelines III. Wrist. 2010.

28.   Patel M. Wrist laceration (ultrasound) [Internet]. Radiopaedia.org. 2021 [cited 2023 Nov 6];Available from: https://radiopaedia.org/cases/86723

29.   Patel M. Carpal tunnel syndrome [Internet]. Radiopaedia.org. 2018 [cited 2023 Nov 8];Available from: https://radiopaedia.org/cases/63771

30.   Patel M. Scaphotrapezial joint ganglion cyst [Internet]. Radiopaedia.org. 2021 [cited 2023 Nov 9];Available from: https://radiopaedia.org/cases/95326

31.   Beggs I, Stefano Bianchi U, Angel Bueno S, et al. European Society of MusculoSkeletal Radiology Musculoskeletal Ultrasound Technical Guidelines IV. Hip. 2010.

32.   Normal Ultrasound Anatomy of the Musculoskeletal System. Springer Milan; 2012.

33.   Wu WT, Chang KV, Lin CP, Yeh CC, Özçakar L. Ultrasound imaging for inguinal hernia: a pictorial review. Ultrasonography 2022;41(3):610–23.

34.   Patel M. Adductor longus tear [Internet]. Radiopaedia.org. 2021 [cited 2023 Nov 9];Available from: https://radiopaedia.org/cases/90111

35.   Jones J, Cid Barría L. Hip joint septic arthritis (ultrasound) [Internet]. Radiopaedia.org. 2021 [cited 2023 Nov 9];Available from: https://radiopaedia.org/cases/86091

36.   Alkhateeb K. Acetabular labral tear hip [Internet]. Radiopaedia.org. 2019 [cited 2023 Nov 16];Available from: https://radiopaedia.org/cases/72216

37. Petersilge CA. Chronic Adult Hip Pain: MR Arthrography of the Hip. RadioGraphics 2000;20(suppl_1):S43–52.

38. Chmiel-Nowak M, Schubert R. Acetabular labral tear [Internet]. Radiopaedia.org. 2011 [cited 2023 Nov 16];Available from: https://radiopaedia.org/articles/14047

39. Beggs I, Stefano Bianchi U, Angel Bueno S, et al. European Society of MusculoSkeletal Radiology Musculoskeletal Ultrasound Technical Guidelines V. Knee. 2010.

40. Patel M. Quadriceps tendon tear [Internet]. Radiopaedia.org. 2011 [cited 2023 Nov 9];Available from: https://radiopaedia.org/cases/12805

41. Bickle I, Patel M. Tenosynovial giant cell tumour (knee) [Internet]. Radiopaedia.org. 2019 [cited 2023 Nov 9];Available from: https://radiopaedia.org/cases/71989

42. Patel M. Deep infrapatellar bursitis [Internet]. Radiopaedia.org. 2021 [cited 2023 Nov 9];Available from: https://radiopaedia.org/cases/86278

43. Beggs I, Stefano Bianchi U, Angel Bueno S, et al. European Society of MusculoSkeletal Radiology Musculoskeletal Ultrasound Technical Guidelines VI. Ankle. 2010.

44. Patel M. Anterior talofibular ligament injury [Internet]. Radiopaedia.org. 2019 [cited 2023 Nov 9];Available from: https://radiopaedia.org/cases/66965

45. Patel M. Achilles tendon tear [Internet]. Radiopaedia.org. 2020 [cited 2023 Nov 9];Available from: https://radiopaedia.org/cases/76966

46. Patel M. Peroneus brevis tear [Internet]. Radiopaedia.org. 2023 [cited 2023 Nov 9];Available from: https://radiopaedia.org/cases/168567

47. Bureau NJ, Ziegler D. Economics of Musculoskeletal Ultrasound. Curr Radiol Rep. 2016;4(8).